

2. LITERATURE REVIEW

2.1. Silk and its aspects

Textile and textile industry is a branch of industrial science that deals with flexible material synthesized by forming an interlocking network of either natural or synthetic fibres or both together. The flexible material used in textile industry has diverse source of origin *viz.* plant (jute, cotton, flax, hemp, bamboo), animal (silk, wool), mineral (glass fibre, asbestos) and synthetic (Kevlar, rayon, acrylic, spandex, nylon, polyester). In the last two decades, China has emerged as largest producer and exporter of textile throughout the globe. India ranks third after European Union (28 countries) with an export value of approximately 17 billion U.S. dollars (Sabanoglu 2020).

India and Indian culture bears a traditional inheritance of textile, specially the segment that deals with handicrafts and was considered as “golden bird” before time to time exploitation by foreign invaders (Dixit and Lal 2019). Since 2004, Indian textile and clothing industry showed a positive trend of growth covering ~14% and ~11% industrial product and countries export basket respectively. Textile industry in India generates employment to more than 45 million peoples with greater percentage of women’s than man (Tandon and Eswara Reddy 2013). Among different section of textile industries, maximum employment was generated in the sector of silk where India stood 2nd in world ranking after China contributing ~13% of the total (Bukhari and Kour 2019).

Due to prevalence of diverse geographical locations and environmental gradient India produces all forms of silk *viz.* mulberry, tasar, eri and muga. Throughout the globe, silk is produced in more than 40 countries, out of which India and China contributes the bulk amount (more than 90%) (Bukhari and Kour 2019). In India, the states of Karnataka, West Bengal, Andhra Pradesh and Tamil Nadu contribute ~90% of the total annual production of silk textile (Fig. 1). Beside this, the states of Bihar, Assam, Jammu and Kashmir, Madhya Pradesh, Manipur and Meghalaya also contributes a significant portion in the growth of silk industry (Bhat and Choure 2014).

Silk industry was broadly divided into two type's viz. mulberry and vanya (wild) silk (Ram et al. 2020). Vanya silk are mostly distributed in remote sterile regions such as high altitude of hills and in core of forest areas of China, India, Burma, Korea and parts of Africa (equatorial region) and South-East Asia. Tasar, eri and muga are the principal contributing component of vanya silk, with tasar accounting more than 90% of the total non-mulberry silk distribution on global platform (Bukhari et al. 2019). In India non-mulberry silk rearing practice was traditionally being carried out by tribal peoples, as it provides a permanent earning source throughout the year (Sharma 2019).

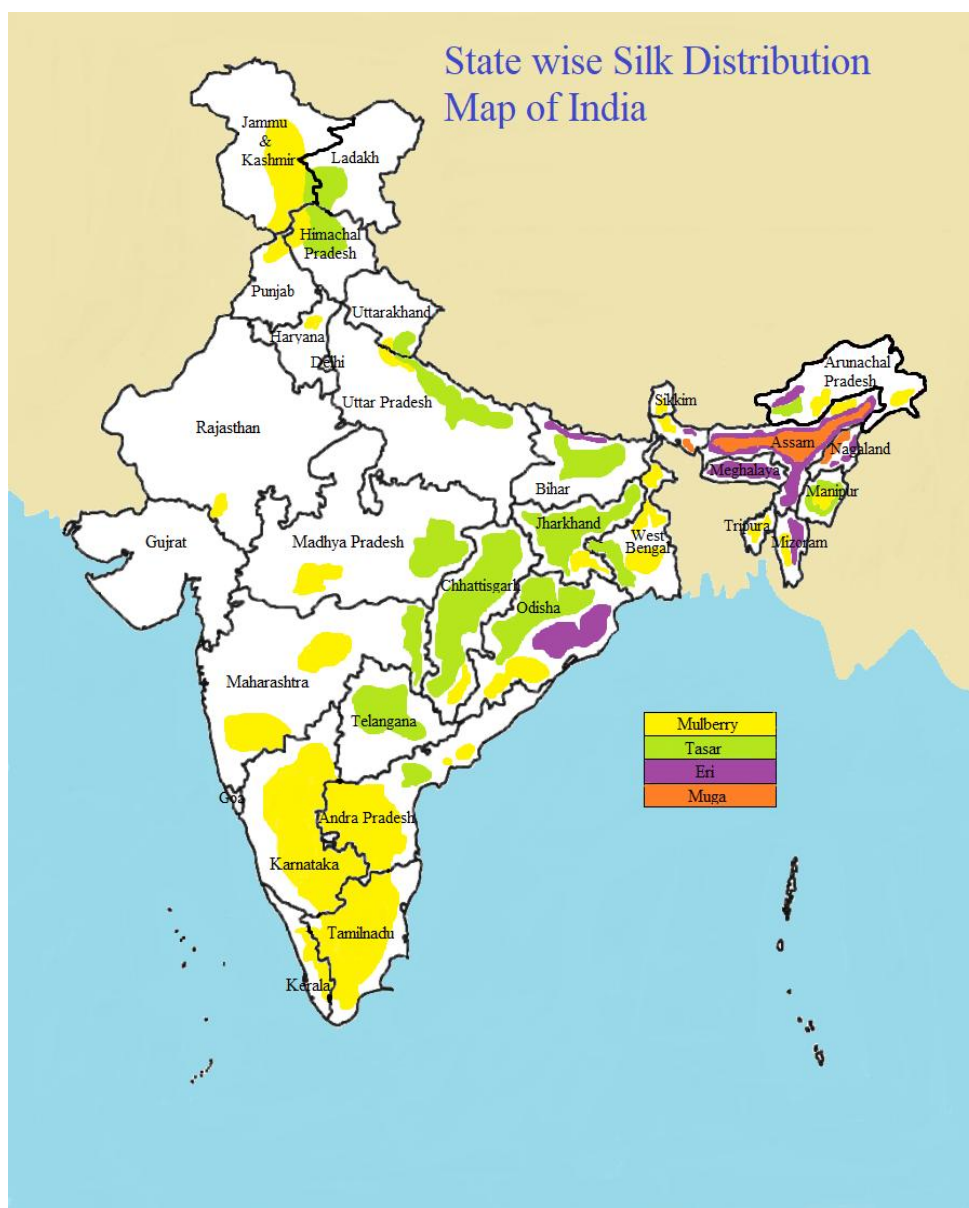


Fig. 1: State wise distribution map of different forms of silk in India

2.1.1. Vanya (wild) silk

Tasar silk, commonly known as “Kosa silk” is traditionally practiced in India by the tribal of present Jharkhand state (Vigneswaran et al. 2015), more specifically by the conventional local peoples of Chotanagpur region are their successive inventers (Bhatia and Yousuf 2014). The fibre length of tasar is short, which makes it more durable than cultivated silk (Vigneswaran et al. 2015). India is the largest exporter of tropical tasar produced by the silkworm *Antheraea mylitta* (Lepidoptera: Saturniidae). Another form of tasar found in India is oak tasar (temperate tasar), which is superior to tropical tasar (Vepari and Kaplan 2007). Different species of oak tasar viz. *Antheraea proylei* (India), *Antheraea yamamai* (Japan) and *Antheraea pernyi* (China) are found in different parts globe with china being largest producer and distributor of it. In India, tropical tasar is basically produced in different parts of the state of Jharkhand, Orissa, Chhattisgarh, Maharashtra, West Bengal and Andhra Pradesh, while oak tasar is produced in the different parts of Manipur, Uttar Pradesh, Himachal Pradesh, Meghalaya, Assam, Ladakh and Jammu and Kashmir. Tropical tasar has wide range of host plants starting from *Terminalia alata*, *Terminalia arjuna* and *Shorea robusta* as primary host; *Lagerstroemia parviflora*, *Anogeissus latifolia*, *Ziziphus jujube*, *Terminalia bellerica* and *Syzygium cumini* as most common secondary host available naturally in the forests of Indian tropical tasar belt; whereas species like *Artocarpus lakoocha*, *Bauhinia variegata*, *Bombax ceiba*, *Buchanania latifolia*, *Canthium didymium*, *Lecythidaceae*, *Carissa carandas*, *Celastrus paniculatus*, *Chloroxylon sweitenia*, *Dalbergia sissoo*, *Diospyros lanoxylon*, *Dodonea viscosa*, *Embelica officinalis*, *Ficus bengalensis*, *Ficus benjamina*, *Ficus hispida*, *Ficus religiosa*, *Ficus retusa*, *Ficus tsjakela*, *Gardenia lucida*, *Garuga pinnata*, *Lagerstroemia indica*, *Lagerstroemia speciosa*, *Madhuca indica*, *Melastoma malabathricum*, *Messua ferrea*, *Prynus domestica*, *Pterocarpus marsupium*, *Rhizophora caseolaris*, *Semecarpus anacardium*, *Shorea talura*, *Syzygium cumini*, *Tectona grandis*, *Terminalia bellerica*, *Terminalia catappa*, *Terminalia chebula*, *Terminalia paniculata*, *Zizyphus rugosa* and *Zizyphus xylopyrus* are the tertiary host plant for tropical tasar (Jena 2016). The most common primary host plant of oak tasar (temperate tasar) are *Lithocarpus dealbata*, *Quercus incana*, *Quercus himalayana*, *Quercus leucotrichophora*, *Quercus floribunda*, *Quercus griffithi*, *Quercus semicarpifolia* and *Quercus serrata*, commonly found in

high altitudinal belt. While species like *Castanopsis indica*, *Castanopsis lancaefolia*, *Castanopsis purpurella*, *Lithocarpus fenestrata*, *Quercus baloot*, *Quercus glauca*, *Quercus kamroopi*, *Quercus lamellose*, *Quercus lanata*, *Salix viminalis* are commonly recognised as secondary host of temperate tasar (Tikader and Kamle 2010). In the five year tenure from 2015-2019, in India maximum tasar silk production of 3268 MT was noted in the year 2016-17 (Table 1). In the last five year tenure a gradual uniform tasar production rate was noted with slight up or down that can be neglected on a broader scale.

Table 1: Vanya silk production in India for the year 2015 to 2019

Year	Raw silk production (MT)			Total Vanya Raw Silk (MT)
	Tasar	Eri	Muga	
2019-20	3136	7204	241	10581
2018-19	2981	6910	233	10124
2017-18	2988	6661	192	9841
2016-17	3268	5637	170	9075
2015-16	2819	5060	166	8045

(Source: Central Silk Board; <http://csb.gov.in>)

Eri silk, is popular in India as “Assam silk” (Sarkar 1988). The term “eri” has derived from the Assamese word ‘era’, denoting plant of castor oil that serves as primary food plant for the eri silkworm. Eri silk is produced from the fibre of the cocoon produced by the silkworm *Philosamia ricini* ((Lepidoptera: Saturniidae). The cocoon of eri remains open at one end and thus it cannot be reeled for producing yarn of continuous filament, as that practiced for cocoons of other silkworms viz. tasar, muga and mulberry (Jolly et al. 1979). Among Indian states, Assam ranks first in terms of eri silk production followed by Meghalaya, Nagaland, Orissa, Arunachal Pradesh, Mizoram and West Bengal. In north-east India, seven eco-races viz. Borduar, Dhanubhanga, Sille, Titabar, Nongpoh, Mendipathar and Kokrajhar are very popular in terms of eri silk production, among them cocoon produced from Kokrajhar was brick red in colour, while white colour cocoon is produced from other eco-races (Chattopadhyay et al. 2018). Eri silkworm is a polyphagous and multivoltine species that feeds upon more than 29 diversified host leaves (Reddy et al. 2002). Most of eri host plants umbels under the family families Euphorbiaceae, Araliaceae, Simaroubaceae and Apocynaceae. *Ricinus communis* (castor) and

Heteropanax fragrans (kesseru) are the primary host plant of eri silkworm. Kumar and Gangwar (2010) reported that eri cocoon produced during spring by feeding leaves of castor was the most superior quality eri silk. Although on the basis of feeding preference by eri silkworm prefers both castor and kesseru, but it has been reported that eri silkworm produces better quality cocoon on feeding castor (Singh et al. 2011). Beside primary host plant species like *Manihot esculenta*, *Evodia fraxinifolia*, *Ailanthus grandis*, *Ailanthus excelsa* serves as secondary host plant for eri silkworm. In some eri culture zone combination of *Manihot esculenta* (tapioca) with castor and kesseru was supplemented to the silkworm and it was reported that mixed supplementation has no effect over eri cocoon quality (Deka et al. 2011; Patil et al. 2009). The species like *Ailanthus glandulosa*, *Ailanthus tryphysa*, *Artocarpus heterophyllus*, *Carica papaya*, *Celastrus monospermus*, *Cinnamomum cecicodaphne*, *Ficus benghalensis*, *Gmelina arborea*, *Hodgsonia heteroclite*, *Jatropha curca*, *Jatropha multifida*, *Micromelum pubescens*, *Oroxylum indicum*, *Plumeria rubra*, *Sapium eugenifolium*, *Sapium sebiferum*, *Zanthoxylum alatum*, *Zizyphus mauritiana*, *Mechelia champaca*, *Spathodea companuclata* also has been reported to serve as host plant for eri silk work, and thus can be considered as tertiary host plant (Das et al. 2020). According to the report of Central Silk Board (CSB), India it was observed that a gradual increase in eri silk production rate was noted in between the period 2015-2019. An increased rate of ~42% was noted in raw eri silk production in the year 2019-20 in comparison to 2015-16.

Muga silk is produced from the cocoon of the larvae *Antheraea assamensis* which remains confined (endemic) to north-east India, more specifically in the Brahmaputra valley in Assam (Tikader et al. 2013). The state of Assam holds monopoly in muga silk production accounting more than 95% of total muga silk production in the country. The “Golden Muga” silk of Assam is endemic to the state and was the monopoly distributor throughout the world (Goswami et al. 2015). Muga rearing practice was reported to be most fruitful under temperature range of 20 – 31°C, maintaining humidity around 65 – 95%, and this environmental condition prevails in entire north-east India (Tikader et al. 2013). Traditionally muga culture was carried as outdoor practice, but gradually it has been acclimatised as semi-domestic rearing practice where rearing is carried out as outdoor practice, while cocoon formation and grainage is carried out as indoor practice (Barman and Rajan 2012). In has been

reported that on conducting outdoor practice, abiotic factors like strong wind, rainfall, soaring temperature and climate change and biotic factors like pests, predators and pathogens causes heavy loss to muga silkworm specially in the first three instars (Thangavelu et al. 1988). Sengupta et al. (1992) reported that abiotic factors are mostly responsible for larval loss and most of the loss occurs in the early stage of growth. To overcome the all season loss muga practitioners gradually shifted towards indoor practice. Different indoor rearing technique has been proposed by different workers, some of them are still followed. Significant retention of effective rate of rearing has been proposed by Thangavelu and Sahu (1986) when indoor practice was carried out with soalu plant. Similarly iron tray method of Bhuyan et al. (1991) also reported significant retention of effective rate of rearing where iron tray covered in sand bed with slotted cover containing som twigs as food supplementary material. Among the host plant of muga silkworm *Persea bombycina* (som) and *Litsea monopetala* (soalu) is the primary host, while species like *Cinnamomum camphora*, *Cinnamomum tamala*, *Litsea citrate*, *Litsea salicifolia* are the common secondary host plant (Bhattacharya et al. 1993). Other species like *Actinodaphne augustifolia*, *Actinodaphne obovata*, *Celastrus monosperma*, *Cinnamomum cecicodaphne*, *Cinnamomum obtusifolium*, *Gmelina arborea*, *Litsea nitida*, *Machilus odoratissima*, *Michelia champaca*, *Michelia oblonga*, *Symplocos grandiflora*, *Symplocos ramosissima* are also reported to act as occasional host plant of muga silkworm (Das et al. 2020). In the five year tenure from 2015-2019 a gradual increase in muga raw silk production has been reported by CSB. Currently on an average 240 MT of raw muga silk is been produced by India in a year.

2.1.2. Mulberry silk

Silk that was first discovered in China around 2200 B.C. most probably in the period of Chou King has taken several decades to perpetuate in other parts of the world. Some study also claims Indus civilizations as the prisoner founder of silk (Good et al. 2009). Korea and Japan were the pioneer landmass that learnt the basic concept of silk production from China. In India, traditionally silk production was practiced by the peoples of foot-hill regions of Himalaya (Tuigong et al. 2015). British East India Company first started commercialization, trading and exporting Indian silk across the globe and established the basic platform which today leads to the formation of 2nd largest silk industry in the world.

Among all naturally occurring basic forms of silk, mulberry silk contributes ~90% of the total raw silk produced globally. Mulberry silk was produced from the cocoon of the silkworm (*Bombyx mori*), that was traditionally native to China. On the perspective of silkworm, at the end of larval fifth instar, silk cocoon is synthesized by the worm to protect itself from adverse environmental condition including natural calamities, along with biogenic agents like microbes and predators, so that they can metamorphose into moth without any disturbance (Nivedita and Sivaprasad 2014). Mulberry silk is an elastic, highly tensile, highly tough organic polymer synthesized inside the silk gland of the insect (Li et al. 2020). Silk, mostly mulberry silk is considered as “queen of textiles” because of its mechanical strength, flexibility, durability, dyeability and tactile properties, and the comfort level it provides to the skin on wearing silk based garments (Nguyen et al. 2019). The silk gland is a typical exocrine gland that remains rudimentary till the 4th instar of silkworm larvae. With the onset of 5th instar the silk gland begins to developed which on full maturation retains ~40% total weight of the larvae (Kunz et al. 2016). On the basis of functional and structural differences, silk gland can be segmented into three parts viz. anterior, middle and posterior silk gland. The anterior silk gland is the excretory duct that spinets the silk. The middle silk gland is ~7 cm in length containing ~300 cells that synthesizes mainly the sericin polypeptides, while fibroin is synthesized by ~500 posterior silk gland cells (Dhawan and Gopinathan 2003; Akai 1983). Basically, the silk gland of silkworm contains two principal protein polymers viz. fibroin (~70%) and sericin (~30%) (Gamo et al. 1977). Structurally two threads of fibroin, synthesized by posterior silk gland were crossed linked by sericin, produced from middle silk gland (Chen et al. 2019). Basically sericin is a hydrophilic glycoprotein that forms the outer coat around the fibroin fibres, the hydrophobic glycoprotein core protein (Sinothara et al. 1971). The shielding potentiality of the sericin was due to the presence of large number of hydroxyl amino acids that are capable of forming interconnecting hydrogen bonds (Sahu et al. 2016). Fibroin is a heterodimeric protein consisting of 395 KDa heavy chain and small subunit of 25 KDa linked by disulphide bond at the carboxylic end (Zhou et al. 2000). The large and small subunit of fibroin through hydrophobic interactions remains associated with a 25 kDa polypeptide, product of the gene P25 (Tanaka et al. 1999). Crystallographic analysis has reported two types of fibroin so far, one is crystalline β -sheeted phase and the other is semi-crystalline or non-crystalline phase (Lotz and Colonna-Cesari

1979). Sericin polypeptides contains 18 different amino acids with high proportion of two amino acids namely serine (~4%) and glycine (~16%) and it bears a wide variability in molecular weight which may be as low as 24 KDa or as high as 400 KDa (Tokutake 1980). Takasu et al. (2002) through SDS-PAGE analysis reported that sericin protein isolated from silk gland varies in their molecular weight *viz.* 250, 400, 150 KDa respectively. Same study also reported similarity in amino acid sequence of 400 and 150 KDa sericin proteins, which is the indicative signal of presence of different coding gene for 250 KDa sericin obtained from middle silk gland. Structurally sericin contains amalgamation of two protein structures *viz.* random coil (63%) and β -sheet (35%) respectively.

Traditionally during industrial processing of the cocoon a significant portion of the sericin gets dissociated from the silk fibre and has been discarded (Kundu et al. 2008). Gulrajani (2005) reported that 50,000 tons of sericin was present in 400,000 tons dry cocoons produced across the globe. It has been identified that sericin that generally gets discarded from silk industry bears wide range of nutraceutical and cosmeceutical properties. Mondal et al. (2007) reported that in many cosmetic industry sericin acts as an active ingredient in the manufacture of face masks, anti-ageing creams, sunscreen lotions, moisturizers and shampoos. Due to the presence of considerable amount of antioxidant activity sericin is used in the suppression of occurrence of colon tumors (Zhaorigetu et al. 2001). It has been proposed through rat modelling that sericin supplement increases the intestinal absorption and thereby bioactivity of some essential elements like Fe, Zn, Mg and Ca (Sasaki et al. 2000). Beside this it has also been reported that consumption of sericin fibre is effective in the treatment of constipation (Sasaki et al. 2000). Due to the presence of functional groups like $-\text{OH}$, $-\text{COOH}$ and $-\text{NH}_2$ in the peptide chain of sericin it is often considered in the process of bioconjugation and drug delivery (Zhang et al. 2006). Beside this in the manufacture of sportswear, sericin is used as it bears the potentiality to evaporate the absorbed sweat (Morooka et al. 2006). It is also used in the manufacture of surgical wound-dressing material containing less than 10% crystallinity (Tsubouchi 1999). Beside this, biocompatible silk fibroin is also reported to be used in medical and garment industry for the manufacture of gloves, neck braces, wrist and knee bands, knitted socks and innerwear (Nivedita and Sivaprasad 2014). Due to the prevalence of less mechanical friction, application of

fibroin based wound dressing materials are increasing in medical industry, as it promotes early healing and do not peel-off the newly formed skin during removal or dressing (Mondal et al. 2007). Silk fibroin protein has been reported to be useful in gene targeting in the delivery system of drugs and proteins (Nguyen et al. 2019). Byun et al. (2010) reported the application of γ -irradiated silk fibroin in the treatment of tumour. Inouye et al. (1998) reported the use of silk fibroin in animal cell culture as a substitute of collagen, as it provide base for cell adherence and proliferation (Jin et al. 2004).

The quality of silk produced depends upon the race of silkworm selected for rearing. Literature survey reports maintenance of ~400 different races of silkworm (*Bombyx mori*) in different parts of the world, mostly by the traditional silk rearing countries viz. India, China, South Korea, Japan, France and Italy (Srivastava et al. 2011). In nature three types of silkworm prevails viz. univoltines, bivoltines and multiivoltines categorized on the basis of number of life cycle the worm completes in a year. Univoltine and bivoltine silkworms completes one and two life cycle in a year respectively, whereas multivoltine silkworms completes on an average 4-5 life cycle in the same tenure. Thus on the basis of production quantity, multivoltine silkworms are mostly preferred. However on the basis of superiority of cocoon production, bivoltine silkworms lead the ranking (Kamble et al. 2007). Traditionally in India different races of silkworm were reared in different geographic locations (Table 2) viz. Nistari (West Bengal), Pure Mysore (Karnataka) and Sarupat and Moria (Assam) (Chatterjee et al. 1993). In India the quality of silk produced is quite low probably because of two factors, (i) greater practice of multivoltine silkworm rearing and (ii) prevalence of tropical climatic conditions (high temperature with low humidity) mostly across the country. For improving quality of silk in the last few decade's attempts has been taken by breeders to develop bivoltine and hybrid silkworm breeds (Lakshmi et al. 2011). The tropical environmental condition of India favours the development of cross-breed (multivoltine \times bivoltine), and the developed cross-breed showed better survival and reproductive ability, but the major drawback was the production of inferior quality cocoon which often gets rejected in the international market (Singh et al. 2010). With an aim to develop superior quality cocoons, attempts were made by breeders of different Central Sericultural Research and Training Institute (CSR&TI), India to develop hardy silkworm races. Breeding

of bivoltine breeds was first introduced in India in 1955 by Harada by the development of KA (Kalimpong A) breed (Ramesh Babu et al. 2005).

Table 2: Indigenous silkworm races in India

Name of the Race	Voltine Nature	State of Rearing	Cocoon Colour	Cocoon Shape	Comment
Nistari	Multivoltine	West Bengal	Golden yellow	Spatulate	Introduced in India around 1788 in Madras and then spread in Bengal
Pure Mysore	Multivoltine	Karnataka	Greenish yellow	Oval	Common in Western Ghats and is considered as hardy and disease resistance race
Sarupat	Multivoltine	Assam	White	Spatulate	Endemic to Assam
Moria	Multivoltine	Assam	White	Spatulate	Endemic to Assam
Barapolu	Univoltine	West Bengal	Greenish white or pure white	Oval	Race is degenerated
Kashmiri race	Univoltine	Kashmir	Yellow	Oval	Race is degenerated

Most of the commercial hybrids of silkworm were predominantly developed through a cross between multivoltine (♀) × bivoltine (♂). The hybrids developed in the breeding programme of CST&TI showed high survival, low disease incidence, superior cocoon parameters and raw silk recovery. The developed bivoltine hybrids displayed long filament length, less deviation in size and high tensile strength. The F1 hybrids have gained considerable attention of Indian farmers because of their high commercial yield. The supremacy of F1 hybrids was documented by comparing their yield with their parental line. For the development of high quality, productive silk the silkworm hybrids recognized by Central Silk Board in India are enlisted in Table 3. With the introduction of cross-breed in India the annual mulberry silk production has increased and the last few years it has reached the production mark of ~25000 MT per year (Table 4). Beside breeds of silkworm, production of good quality silk depends upon quality of mulberry leaves the larvae fed upon. All essential nutrients and internal moisture content present inside mulberry leaves are required by the larvae for proper growth and development (Hamamura 1959). Dong et al. (2017) reported co-evolutionary mode of development between silkworm and mulberry that ultimately results in the development of superior cocoon yielding good quality raw silk. Probably the process of natural selection has selected mulberry leaf as best food source of silkworm larvae. Mulberry leaves as

supplement act as sole source of carbohydrates, lipids, proteins, inorganic matter, vitamins and moisture (Masthan et al. 2017). The leaves (mulberry) nutrient content varies subsequently with season, age, variety and nature of harvesting (Sarkar 2020). For improving silk quality, attempts has been made time to time to supplement silkworm larvae with other source of food which failed to provide desired result, possibly due to physiology of digestion and thereby assimilation inside body of larvae does not support alternative food source (Manjula et al. 2021). Lalfelpuii et al. (2014) stated that physiological performance of silkworm larvae is directly proportional to the digestion and assimilation efficiency of the leaf they fed upon. Thus out of the total mulberry leaves consumed, the quantity of leaves digested and nutrient incorporated by the larvae have a direct effect on silk gland development and cocoon spinning ability (Ruth et al. 2019). Improper nutritional balance hampers larval metabolic activity, resulting in the formation of poor, inferior quality cocoon. Thus attempts has been made by researchers to developed good quality high yielding mulberry cultivars, suitable for silkworm rearing, which will led to the production of silk fibres in the form of cocoon effective from both quality and quantity point of view.

Cultivation of mulberry in a particular geographical area depends upon number of factors including environmental condition, soil moisture content, parental line of the tree including its nutritional status, harvesting procedure, disease management strategy (Sori and Gebreselassie 2016). Mulberry cultivation holds ~16% cost share of the entire cost of silk production (Zhao et al. 2009). Before the development of commercially high yielding varieties of mulberry, cultivation of local varieties that are generally practiced were Kajli and Bombai in West Bengal; Mysore local, Boodi-ranginakaddi and Bilidevalaya in Karnataka. These varieties have low leaf yield (~5-7 and ~10-12 tons ha⁻¹ year⁻¹ under non-irrigated and irrigated conditions respectively) and moisture content (< 65%) and are adapted under harsh / stress conditions. For improving yield and adaptability under wide environmental condition, high yielding region specific varieties were developed and introduced in commercial practice. The region specific developed varieties are S1, S1635, S-146, BC259, C1730, C-776, Tr-10, Tr-4 and many more for Eastern and North Eastern region of India; AR-11, AR-12, G-2, G-4, RF5135, RF5175, RC-1, RC-2, S-13, S-34, S-36, Sahana, K2, V1 and many more for Southern region of India. These high

Table 3: Different hybrid lines of silkworm developed and reared in India

Nature of Cross	Hybrid	Season of Rearing	State of Rearing
Multivoltine × Bivoltine	APDR15 × APDR115	Spring, summer, autumn, winter	West Bengal, Karnataka
	APM2 × APDR105	Spring, summer, autumn, winter	West Bengal, Andra Pradesh, Karnataka, Tamil Nadu
	APM3 × APS12	Spring, summer, autumn, winter	West Bengal, Karnataka
	BL67 × CSR19	Spring, summer, autumn, winter	Assam, West Bengal, Andra Pradesh, Bihar, Orissa, Jharkhand, Chattisgarh, Uttar Pradesh, Karnataka
	BL67A × CSR101A	Spring, summer, autumn, winter	Andra Pradesh, Karnataka, Tamil Nadu
	MCON1 × BCON4	Spring, summer, autumn, winter	West Bengal, Jharkhand, Andra Pradesh, Karnataka, Tamil Nadu
	MCON4 × BCON4	Spring, summer, autumn, winter	Assam, West Bengal, Orissa, Jharkhand
	MH1 × CSR2	Spring, summer, autumn, winter	Uttar Pradesh, Andra Pradesh, Karnataka, Tamil Nadu, Orissa
	MY1 × NB18	Spring, autumn	Assam, West Bengal, Bihar, Jharkhand, Orissa, MP
	Mysore × CSR2	Spring, summer, autumn, winter	Andra Pradesh, Karnataka, Tamil Nadu
	N × (NB18 × P5)	Spring, autumn	Assam, West Bengal, Bihar, Orissa, MP, Chattisgarh
	N × YB	Spring, summer, autumn, winter	West Bengal
	P2D1 × NB18	Spring, summer, early autumn	Assam, Andra Pradesh, West Bengal, Bihar, Orissa, Jharkhand, Chattisgarh, Uttar Pradesh, Uttarakhand
	PM × CSR2(SL)	Spring, summer, autumn, winter	Assam, Andra Pradesh, Maharastra, Tamil Nadu, Karnataka
	PM × NB18	Summer	Assam, Bihar, Orissa, MP
RD1 × NB18	Summer, early winter	Uttar Pradesh, Uttarakhand	
Varuna (BL24 × C.NICHI)	Spring, summer, autumn, winter	Andra Pradesh, Karnataka, Tamil Nadu	
Bivoltine × Bivoltine	APS105 × APS126	Spring, summer, autumn, winter	Andra Pradesh, Karnataka, Tamil Nadu
	APS45 × APS12	Spring, summer, autumn, winter	Tamil Nadu, Jammu and Kashmir
	CA2 × NB4D2	Spring, autumn, early winter	Assam, West Bengal, Bihar, Jharkhand, Orissa, MP, Chattisgarh
	CC1 × NB4D2	Autumn, early winter	Uttar Pradesh, Uttarakhand, Jammu and Kashmir

	CSR2 × CSR4	Spring, rainy	Andra Pradesh, Karnataka, Tamil Nadu
	CSR2A × CSR4A	Spring, rainy	Karnataka, Tamil Nadu
	CSR46 × CSR47	Spring, summer, autumn, winter	Assam, Andra Pradesh, West Bengal, Himachal Pradesh, Orissa, Karnataka, Chattisgarh, Uttar Pradesh, Uttarakhand
	CSR48 × CSR5	Spring, rainy	Karnataka, Tamil Nadu
	DUN17 × DUN18	Spring, summer, autumn, winter	Assam, West Bengal, Himachal Pradesh, Karnataka
	GEN3 × GEN2	Spring, summer, autumn, winter	Assam, West Bengal, Andra Pradesh, Tamil Nadu, Jammu and Kashmir
	KSO1 × NP4	Spring, summer, autumn, winter	Himachal Pradesh, Jammu and Kashmir, Karnataka
	NB18 × P5	Winter	Assam, Bihar, Orissa, MP
	NK2 × NP4	Spring, summer, autumn, winter	Assam, Jharkhand
	PAM101 × NB4D2	Autumn, early winter	Uttar Pradesh, Uttarakhand, Jammu and Kashmir
	PAM111 × SF19	Autumn, early winter	Uttar Pradesh, Jammu and Kashmir
	SH6 × KA	Spring, Winter	Assam, West Bengal, Bihar, Orissa, MP
	SH6 × NB4D2	Spring	Uttar Pradesh, Uttarakhand, Jammu and Kashmir
	SLD4 × SLD8	Spring, summer, autumn, winter	Assam, West Bengal, Andra Pradesh, Tamil Nadu, Jammu and Kashmir
	YS3 × SF19	Spring	Uttar Pradesh, Uttarakhand, Jammu and Kashmir
Multivoltine × Multivoltine	MCON1 × MCON4	Spring, summer, autumn, winter	West Bengal, Andra Pradesh, Karnataka, Tamil Nadu
	N × M12(W)	Summer	West Bengal
	N × MCON4	Spring, summer, autumn, winter	West Bengal, Andra Pradesh, Tamil Nadu
	PM × C110	Spring, summer, autumn, winter	West Bengal
Double hybrid	(CSR6 × CSR26) × (CSR2 × CSR27)	Spring, rainy	Assam, West Bengal, Andra Pradesh, Bihar, Orissa, Jharkhand, Chattisgarh, Uttar Pradesh, Karnataka

(Source: Central Sericulture Research & Training Institute)

Table 4: Mulberry silk production in India for the year 2015 to 2019

Year	Raw silk production (MT)		Total Raw Mulberry silk (MT)
	Bivoltine	Cross breed	
2019-20	7009	18230	25239
2018-19	6987	18357	25344
2017-18	5874	16192	22066
2016-17	5266	16007	21273
2015-16	4613	15865	20478

(Source: Central Silk Board; <http://csb.gov.in>)

yielding varieties have leaf yield of ~12-15 and ~35-70 tons ha⁻¹ year⁻¹ under non-irrigated and irrigated conditions respectively and tissue moisture content of < 75 %. Area covered under mulberry plantation has gradually increased in India and in the last five year (2015 – 2019) a gradual linear plantation rate was observed (Fig. 2).

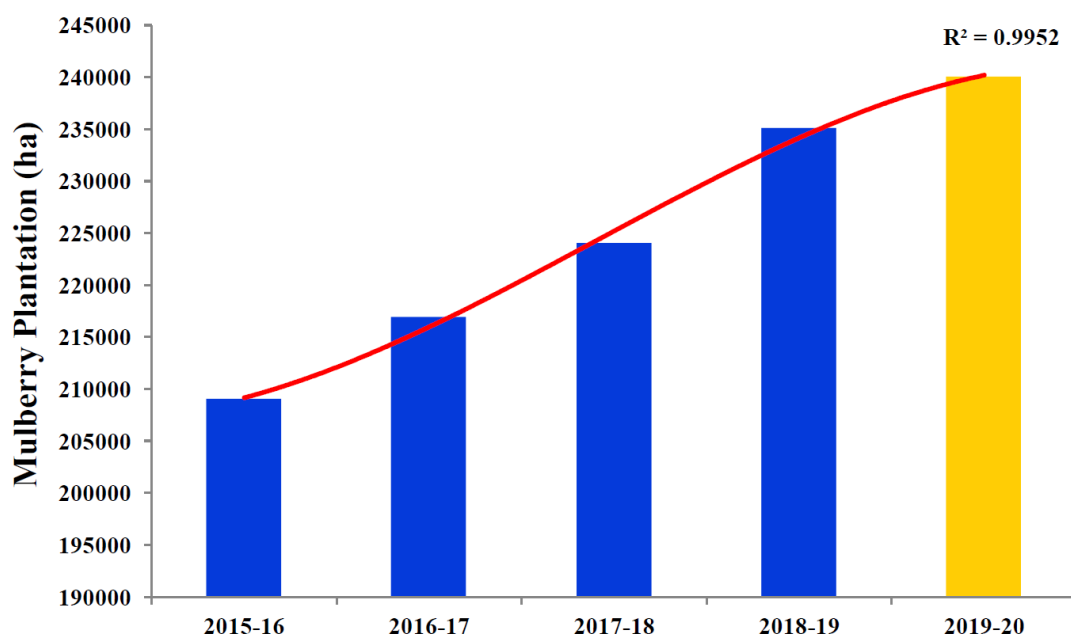


Fig. 2: Graphical representation of mulberry plantation (ha) in India for the year 2015 to 2019

On the basis of morphological (number of leaves, branches; lamina area; leaf yield) and physio-biochemical (moisture, chlorophyll, protein and carbohydrate content) parameters Sinha et al. (2001) reported four commercially selected cultivars of mulberry viz. S1, C763, C776 and K2. Adolkar et al. (2007) on the basis of growth

and yield reported six mulberry cultivars *viz.* S1, S2 and S36, K2, Thailand and Thika. Chaluachari and Bongale (1995) reported S1635 as superior variety over S-13, S-34, S-146, and TR-10 in terms of protein, sugar and moisture contents. S1635 was also recognized as best salt tolerant mulberry genotype among commercially released other salt tolerant genotypes *viz.* S36, S13 and MR2 (Gnanaraj et al. 2011). Kumar et al. (2016) reported that among improved mulberry genotypes, S1635 and TR10 was the best commercially accepted genotype. Debaraj et al. (2010) reported that in north-east India cultivars like V1, S1635, BC259, K2 and S1 are evenly good in terms of leaf and cocoon yield and are better performing than other tested mulberry varieties.

2.1.3. Silk in West Bengal

In West Bengal production of all the four types of silk *viz.* mulberry, tasar, eri and muga was carried out by the farmers, among them practice of mulberry silk covers majority of the proportion. West Bengal ranks 3rd in mulberry silk production with blocks under the district of Malda, Murshidabad and Birbhum were the major contributors (Anonymous 2018). According to the report of Anonymous (2016) currently in West Bengal about 2000 villages are directly involved in sericulture practice with 37,883 acres of land under mulberry plantation.

Throughout the state of West Bengal mulberry silk rearing was practiced except Howrah and East Midnapore district. The rearing practice of tasar silk was carried out in the blocks of the district Bankura, Purulia, Birbhum, Paschim Midnapore and part of Burdwan. While eri and muga silk rearing was mostly practiced in patches of Jalpaiguri, Darjeeling and Coochbehar district (Fig. 3). In West Bengal, tasar silkworm mostly grow on arjun, asan and sal tree, while eri silkworm supplements on castor plant and leaves of Som and Soalu were preferred by muga silkworm. Currently throughout the state of West Bengal 59 technical service centres, 62 basic seed farms, 16 Grainages are present that were established by Directorate of Textiles (Sericulture), Government of West Bengal. Beside this, there are 8 cocoon marketing centres *viz.* Berhampore, Bhadrapur, Panchgram, Sagarpara, Kaliachak, Chanchal, Mothabari and Amrity.

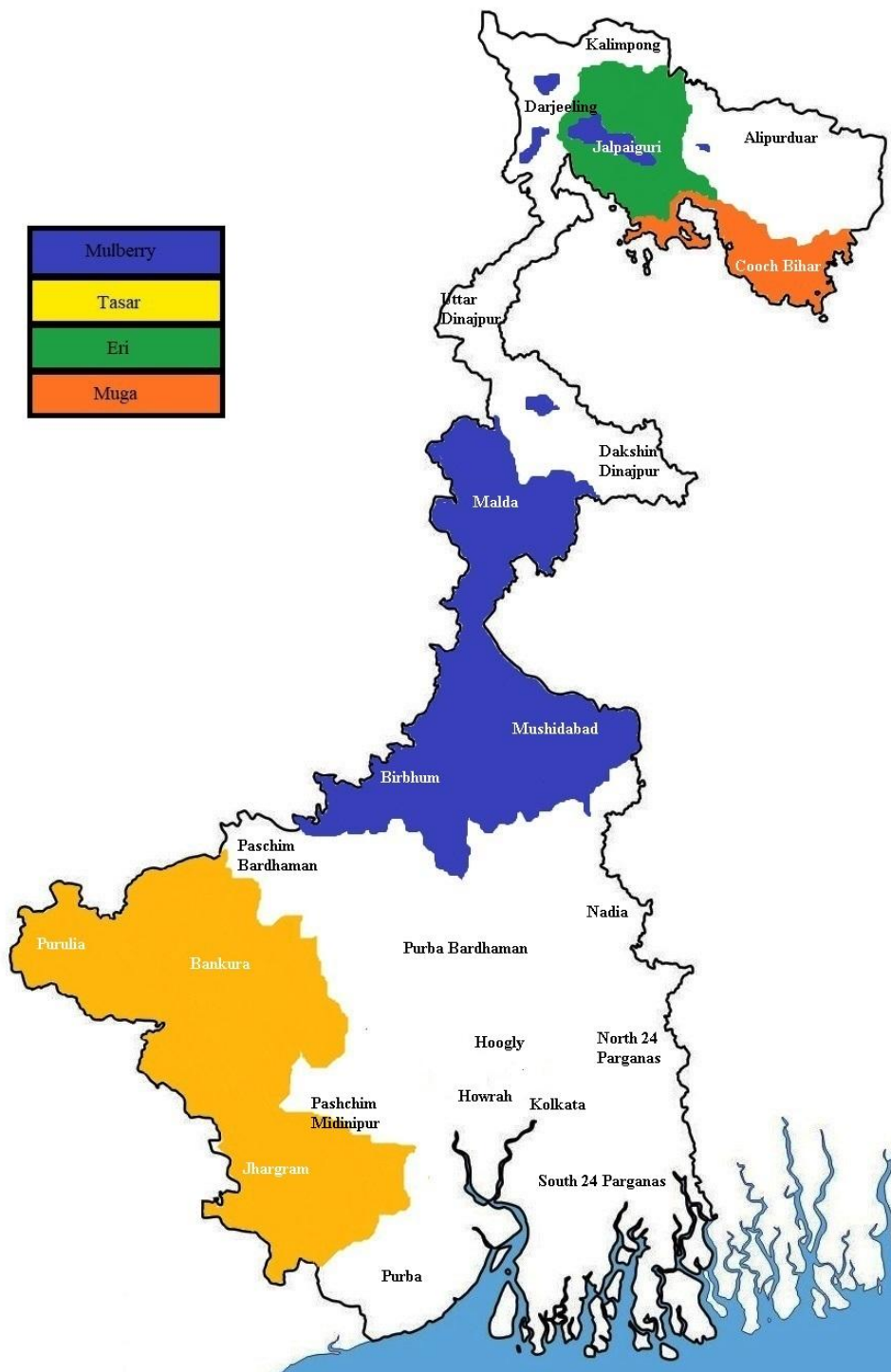


Fig. 3: Major mulberry, tasar, eri and muga silk distribution zones in West Bengal, India

2.1.4. Problems associated with mulberry silk production

India has long traditional history of silkworm rearing and silk production. The agro-based silk industry in India is not well developed throughout the country. The silk farmers often raise their voice in the demand of infrastructure and guidance facility. Time to time different researchers through their survey has highlighted the problems associated with mulberry silk production in India.

Hadimani et al. (2019) has identified major constraints of silk farmers throughout India.

A. The problems associated with mulberry cultivation are:

1. Lack of information about selection of mulberry cultivar according to geographical location and environmental factors.
2. Lack of proper irrigation and drainage facility.
3. Lack of knowledge about the application of bio-fertilizers, VAM and vermi compost for proper growth of the cultivars.
4. Lack of training regarding proper management of plant, including pest and diseases management.
5. High disease incidence and high cost of insecticide and fungicide.

B. The problems associated with silkworm rearing are:

1. Lack of knowledge about proper rearing of crossbred silkworm races.
2. Lack of supply or inconsistent supply of disease free laying (DLFs) from authorized Government sources.
3. Lack of proper rearing and marketing infrastructure in rural areas.
4. Lack of knowledge regarding disease and pests management.
5. Inadequate training facilities from Government sources.

Bukhari et al. (2019) while studying impact and problems of women's in silk industry has identified some common problems of silk industry, prescribed below:

1. Lack of proper separate rearing house for large scale rearing of silkworms.
2. Inconsistency in rearing process (i.e. does not perform rearing practice in every month or season).
3. Lack of sufficient mulberry plantation lands.
4. Land less farmers collect inferior quality leaves from naturally grown mulberry trees which puts impact over rearing process.
5. Lack of guidance and technical knowledge for improving productivity.

Monir and Mandal (2016) has identified major drawbacks in mulberry silk production in West Bengal that puts limitation over production of superior quality silk. The problems faced by agro-based silk industry were:

1. Erratic climatic conditions impacting larval rearing.
2. Cultivation of low yielding mulberry varieties.
3. Improper spacing between two mulberry varieties which limits their proper growth.
4. Rearing of low productive silkworm larvae (Nistari 15-20 kg/dfls) on large scale.
5. High mortality and low productivity on feeding diseased leaves.

2.2. Nanosilver with special reference to green technology

“Nano” is a Greek word signifying anything which is extremely small, and the term “nanoparticles” means clusters of atoms of 1-100 nm in size (Vadlapudi and Kaladhar 2014). Nano is a numerical prefix referring to a billionth i.e. “extremely small” (Ranjit and Baquee 2013). Couvreur (1988) describe nanoparticles as solid, colloidal particles in the size range of 10-100 nm. Nanoparticles are gaining considerable interest in the field of science due to its extensive application in day-to-day life. Due to the presence of catalytic, optical, antimicrobial and anti-carcinogenic properties, nanoparticles have placed itself in a demanding position in the field of biology, electronics and medicine (Lee and Jun 2019). Due to the presence of antimicrobial properties nanoparticles are sometimes considered as nano-antibiotics (Sastry et al. 2003).

Devi et al. (2015) reported that metallic nano particle possesses different physical and chemical properties *viz.* lower melting points, higher specific surface areas, mechanical strengths, specific optical properties. Nanoparticle has exceptionally high surface area to volume ratio and it may be one of the reasons for their extraordinary properties (AbouEl-Nour et al. 2010; Ge et al. 2014). Due to the presence of large surface area the nanoparticle displays characteristics like reactivity, high energy of surface area, absorption, higher solubility, lower melting points and many more (Cadden 1987; Rao and Biswas 2009).

Nanoparticles can be prepared by three means *viz.* physical, chemical and green methods. Physical and chemical methods are not cost-friendly besides this in most of the cases they are toxic in nature and hazardous (Li et al. 2011), due to which they often required purification (Ahmed et al. 2015). Instead of this toxic and hazardous problem, one cannot neglect the increasing demand of nanoparticles in the field of applied science including medicine. A solution to this problem is green synthesis of nanoparticles using reagents that occur naturally in nature such as sugars, vitamins, plant extract, biodegradable polymers, microorganisms etc. as reducing and capping agents (Ahmed and Ikram 2015; Kharissova et al. 2013). Among different types of reducing and capping agents, plant extracts have gained significant importance because of their easy availability and cost effective nature (Sithara et al. 2017). Because of environment friendly nature, nanoparticles synthesized by green technology is widely accepted in many commercial industries like medicine, food, chemical and cosmetic industries (Rao and Gautam 2016). Silver, aluminum, gold, zinc, iron, titanium, palladium and copper are most commonly used metals in the green synthesis of nanoparticles (Vadlapudi and Kaladhar 2014). Among all the metals that are used till date for green synthesis, silver nanoparticles has gained prime focus due to its vast action background which includes good electrical conductivity, chemical stability, catalytic and broad spectrum antimicrobial activity (Sharma et al. 2009). Application of silver nanoparticles was also noted in water treatments (Lu et al., 2016) and water filtration membranes (Haider and Kang 2015).

2.2.1. Nano Technology

Nano technology is an amalgamated technology which combines nano-science with the knowledge from different field of science *viz.* physics, chemistry, biology,

medicines, informatics, and engineering. The concept of nano-science and nanotechnology significantly applies in the application of pharmaceuticals (Jain et al. 2010), biological and chemical sensors (McFarland and Van Duyne 2003), cosmetics, processed food, chemical engineering, high-performance materials, electronics (Chen et al. 2009), precision mechanics, optics (Kelly et al. 2003), energy production, and environmental sciences (Saxena et al. 2012).

2.2.2. Nanoparticles

Nanoparticles are the particle of nano dimension (Nagaich 2016). Nanoparticles can be synthesized with different material having different chemical natures, the most common being metals (Fedlheim and Foss 2001), metal oxides (Naseem and Durrani 2021), silicates (Ehrman et al. 1999), non-oxide (Gan et al. 2021), polymers (Paques et al. 2014; Rao and Geckeler 2011) and organic molecules (Yang et al. 2021). Morphology of nanoparticles varies greatly such as spheres, cylinders, platelets, tubes etc. (Agam et al. 2007). Nanoparticles are used in agricultural field to increase efficiency and productivity of crops (Campos et al. 2014; Nair et al. 2012). Different metabolic pathways in plant can be boost up by the application of nanoparticles (Nair et al. 2011; Giraldo et al. 2014).

2.2.3. Types of Nanoparticles

Based on creation aspect nanoparticles are of two types *viz.* non-engineered and engineered (Kole et al. 2016). Nanoparticles which are derived from the natural events like erosion, forest fire, storm, and volcanic incident are known as non engineered nanoparticles. On the other hand, the nanoparticles that are man made from variety of materials like metals (Ni, Au, Cu, Zn, , Fe and Ag) (Fedlheim and Foss 2001), non-metals (silica) (Ehrman et al. 1999), metal oxides (SiO_2 , CeO_2 , TiO_2 , Fe_2O_4 and Al_2O_3), lipids like stearic acid (Ekambaram et al. 2012) and carbon (fullerene and graphene) are known as engineered nanoparticles. Inorganic non-materials have been extensively used for cellular drug delivery. Shrama et al. (2009) stated that among different inorganic nanoparticles silver nanoparticles draw additional interest because of their novel biological, chemical and physical properties.

2.2.4. Silver and its nano form

Ag (Silver) exist in four oxidation state *viz.* Ag^0 , Ag^+ , Ag^{2+} and Ag^{3+} of which former two are abundant and the remaining two are unstable in aquatic condition (Ramya 2012). Silver if present in metallic form are insoluble in water, but its metallic salts (silver chloride and silver nitrate) are soluble in water. Beside this, silver is not very much toxic to immune, reproductive, cardiovascular system and they are non-carcinogenic in nature.

Silver ion on reduction by suitable reducing agent gets transformed into particles of nano dimension called silver nanoparticle (Dong et al. 2020). Silver nanoparticles are often considered as unique and diversified nano form because of their size, shape, optical (Kelly et al. 2003), electrical (Chen et al. 2009) and magnetic properties (Mwilu et al. 2014). Williams (2008) stated that silver nanoparticles are made up of ~20-15000 silver atoms and their size dimension ranges from 1-100 nm in diameter. Egyptians in ancient time believes that the silver powder has some immense disease resistant and healing properties and they often uses silver powder for the treatment of wound infection (Russel and Hugo 1994). In the manufacture of different industrial product *viz.* textile goods (Perelshtein et al. 2008), plastics, electric appliances, different health care product, silver nanoparticle is often used due to its effective antimicrobial property (Morones et al. 2005). Silver nanoparticles serve as a good source of Ag^+ ions which binds to the bacterial membrane protein forming a pit and also enhances other morphological plasticity (Morones et al. 2005) creating ROS in bacterial cell which ultimately causes bacterial mortality (Yin et al. 2020). Several physical, chemical and biological methods have been used for synthesizing and stabilizing silver nanoparticles (Iravani et al. 2014; Klaus et al. 1999).

2.2.5. Methods for nanoparticle synthesis

A large number of techniques *viz.* laser ablation, gamma and electron irradiation, photochemical methods, microwave processing, chemical reduction and biological synthetic methods has been reported for the synthesis of metallic nanoparticles. There are two broad line methods for nanoparticle synthesis *viz.* top-down method and bottom-up method. In this method large size molecules are broken down into small size molecules which further undergone transformation into particles of nano dimension. Top-down method was often considered as destructive method of nano

synthesis (Iravani et al. 2011). Methods like thermal decomposition, ball-milling, lithography, laser ablation and sputtering comes under top-down method (Ijaz et al. 2020). While in bottom-up method, atoms or molecules aggregate into particles of nano dimension (Chugh et al. 2018). Common bottom-up methods are chemical vapour deposition, sol-gel, spinning and pyrolysis (Ijaz et al. 2020). There are three basic process of nano synthesis *viz.* physical, chemical and biological.

2.2.5.1. Physical methods of nanoparticles synthesis

Different physical methods for nanoparticle synthesis are prescribed below:

a. Thermal decomposition is a common top-down method of nanoparticle formation in which nanoparticles are synthesized by decomposed of concerned material at defined temperature (Salavati-Niasari et al. 2008). Lee and Kang (2004) reported formation of silver nanocrystals through thermal decomposition of silver-oleate complex at 287°C.

b. Pulse laser ablation uses second generation lasers at high intensity to produce plasma inside vacuum chamber. The produced plasma by pulse laser treatment was used to prepare nanoparticles (Satyanarayana and Sudhakar Reddy 2018).

c. Ball-milling method uses mechanical mills of different capacity to generate cost effective and high quantity nanoparticles. The quality of nano particles formed depends upon type, speed, container and grinding medium of the machine. Beside this, control agent used in the process and weight ratio of ball used to powder plays crucial role in determining size of the formed nanoparticles. The major drawback of this process was mechanical limitations which puts hold over formation of ultra-fine particles. Using ball-milling method, zinc oxide (Salah et al. 2011), copper oxide (Yang et al. 2017), titanium dioxide (Yadav et al. 2015) and silver (Khayati et al. 2013) nanoparticles were synthesized.

d. Evaporation–condensation method uses tube furnace and carrier gas phase for nanoparticle synthesis. Using this method, nanoparticles of PbS, Au and Ag have been synthesized (Kruis et al. 2000). In this method the base material is carried by carrier gas to the centre of the furnace for nanoparticle synthesis.

e. Laser ablation synthesizes nanoparticle in liquid environment. Laser irradiation synthesizes silver nanoparticle in pure form by removing other ions, compounds or reducing agents (Lee and Jun 2019). This method is free of any chemical reagents, only mild liquid soluble surfactants are used for proper nano formation (Chen and Yeh 2002).

f. Arc discharge method synthesizes nanoparticles (*viz.* silver nanoparticle) in deionized water without any surfactants using centrifuge separation technique of ions (Tien et al. 2008).

Physical method although gives pure form of nanoparticle but it has certain disadvantage putting a limit over its wide application. Various physical methods have their own disadvantages *viz.* evaporation condensation method consumes large space for tube furnace, consumes higher quantity of energy and thereby increases the environmental temperature and takes longer duration to stabilize the product (Tran et al. 2018); in laser ablation technique prolong exposure time leads to production of high amount of nanoparticles that block the laser path, as a result the laser energy cannot hit the target surface and gets consumed by the already formed nanoparticles (Jamkhande et al. 2019).

2.2.5.2. Chemical methods of nanoparticles synthesis

Chemical synthesis of nanoparticles involves mainly three components *viz.* (a) metal precursors, (b) reducing agents and (c) stabilizing agents (Natsuki et al. 2015). Chemical method of nanoparticle synthesis utilizes chemical reagents like N,N-dimethylformamide (Pastoriza-Santos and Liz-Marzán 2002), sodium borohydrate (Reddy et al. 2009), ethylene glycol (Kim et al. 2006), liquid paraffin and oleylamine (Chen et al. 2007), glucose (Janardhanan et al. 2009), ascorbic acid (Velikov et al. 2003), urea (Lu and Chou 2008) and many more as reducing agents for reducing ionic form of metal to nano form.

Chemical mediated synthesis of nanoparticles has certain disadvantages as it has environmental concerns due to the use of chemicals that are hazardous, along with various harsh reaction parameters and usage of various toxic by-products. The chances of toxic chemicals remaining adhered to the surface of the nanoparticles after synthesis is very high. Moreover, nanoparticles synthesized by this method

tend to get insoluble in aqueous systems or get agglomerated which puts limitation for it to be used in living systems (Borase et al. 2014).

2.2.5.3. Biological synthesis of nanoparticles

Biological or biogenic method uses natural products as reducing and capping agent to form silver nanoparticles (Bhainsa and D'Souza 2006). Recently biological synthesis approaches of silver nanoparticles are emphasized to get relief from complex chemical procedure (Logeswari et al. 2015). In green synthesis, addition of further stabilizing and capping agent from outside is not required, as the natural reagent which is added from plant source contains reducing agent and other cell constituent which acts as stabilizing and capping agents (Srikar et al. 2016). In biological method extracts from different sources *viz.* fungi (Shankar et al. 2003), bacteria (Bahrulolum et al. 2021), plant extract (Zhang et al. 2020) and metabolic bi-products are used for synthesizing nanoparticles.

For biological synthesis of silver nanoparticle, prepared plant extract was added drop wise to the solution of silver nitrate along with continuous stirring (Fig. 4). Garibo et al. (2020) reported the fusion of 2.5 ml extract of *Lysiloma acapulcensis* with 0.001 M silver nitrate for nanosilver biosynthesis. Pirtarighat et al. (2019) reported synthesis of silver nanoparticles by adding extract of *Salvia spinosa* in the ratio of 9:1 to 1 mM silver nitrate, with continuous shaking for 6 hrs at 27°C. Carmona et al. (2017) prepared silver nanoparticles following green technology using 5% *Buddleja globosa* leaf extract mixed with 0.1 to 1 mM silver nitrate solution. Similarly, Krithiga et al. (2015) reported preparation of silver nanoparticles using 5 ml leaf extract of *Clitoria ternatea* and *Solanum nigrum* with 45 ml 0.1 M silver nitrate. The different sources used for silver nanoparticle synthesis are prescribed below.

2.2.5.3.1. Synthesis of silver nanoparticle by algal extract

The biosynthesis of silver nanoparticles by algae gained popularity due to their easy availability in large scale (Balantrapu and Goia 2009). It has been reported that marine algae contain several forms phenolic compounds that acts efficiently as reducing agent (Ibraheem et al. 2016). Beside this, it has been proved that algal extract to some extent displayed antifungal, antibacterial, antiviral properties

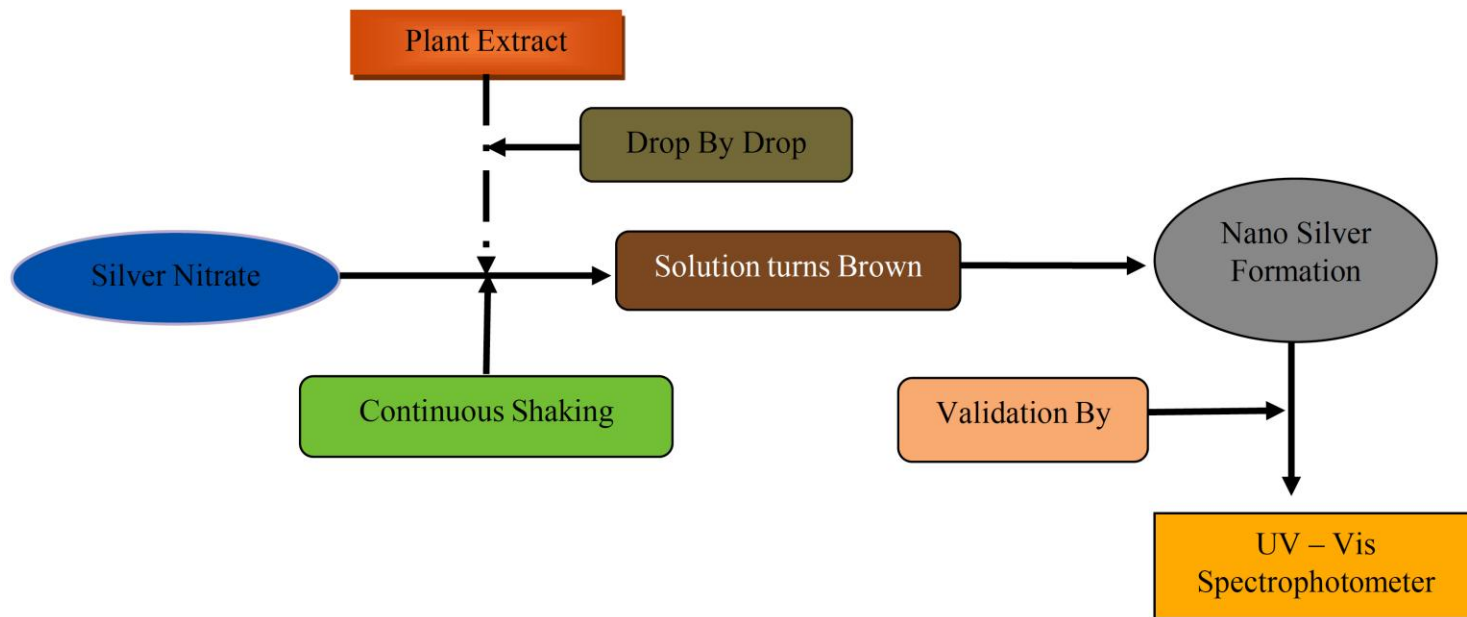


Fig. 4: Sequential steps for green synthesis of silver nanoparticles

(Maneerung et al. 2008). Mainly the marine algae are used for the production of silver nanoparticles (Merin et al. 2010; Kannan et al. 2013). The marine polysaccharides bear reducing as well as stabilizing properties and are reported to provide stability to the synthesized nanoparticles even at moderate pH alteration in presence of electrolytes (Wijesekara et al. 2011). Different algal extracts that are used for the biosynthesis of silver nanoparticles are enlisted in Table 5.

2.2.5.3.2. Synthesis of silver nanoparticles by fungal extract

Fungi have high proliferation rate and are source of large quantity of proteins, acting as reducing and stabilizing agents (Guilger-Casagrande et al. 2019). Fungus mediated biosynthesis of metal nanoparticles can occur by both extracellular and intracellular process. For biosynthesis of nanosilver using fungal extract through extracellular process, at first the fungi were cultured in a liquid medium and then the biomass was transferred in water so that cellular metabolic components get immiscible in water. The water was then filtered, and the filtrate was used for nanosilver synthesis (Ottoni et al. 2017). While in intracellular process, the metal precursor is directly added to the culture of mycelia. The nanoparticles formed were extracted by centrifugation and filtration (Molnár et al. 2018). Different algal extracts that are used for the biosynthesis of silver nanoparticles are enlisted in Table 6.

2.2.5.3.3. Synthesis of silver nanoparticle by bacterial extract

Bacteria serve as a suitable agent for nanoparticle synthesis as they can adapt quickly under different condition and their cultural growth can be controlled by varying temperature and oxygenation, which is helpful for generation nanoparticles of variable size dimension (Mughal et al. 2021). Like fungi mediated nanoparticle synthesis, bacterial mediated nanoparticles can be synthesized by both extracellular and intracellular process. The main drawback of bacterial mediated nanoparticle synthesis was that it cannot put limitation over geometry of nanoparticles under large scale production (Mukherjee et al. 2002). Different algal extracts that are used for the biosynthesis of silver nanoparticles are enlisted in Table 7.

Table 5: Algae mediated synthesis of silver nanoparticles

Algae Name	Extract Used	Characterization	Size (nm)	Shape	Bioactivity	Reference
<i>Padina</i>	Aqueous extract	UV-Vis, FT-IR, SEM, FE-SEM, EDX, XRD	25 - 61.4	Spherical and oval	Prevents proliferation of <i>Staphylococcus aureus</i> and <i>Bacillus subtilis</i>	Bhuyar et al. (2020)
<i>Sargassum myriocystum</i>	Aqueous filtrate	UV-Vis, FT-IR, FE-SEM, HR-TEM, EDX, XRD, SAED	27 -54	Spherical and cubic	Effective against antibacterial, anticancerous and vector born diseases	Balaraman et al. (2020)
<i>Chlorella ellipsoidea</i>	Dry algal powder	UV-Vis, FT-IR, TEM, EDX, XRD, DLS	220.8	Spherical, cubic, triangular, rod, multiply twinned	Effective photo-catalysts for effective degradation of water-soluble pollutants	Borah et al. (2020)
<i>Gracilaria birdiae</i>	Aqueous filtrate	UV-Vis, FT-IR, TEM, DLS	20 - 94	Spherical	Effective against <i>Escherichia coli</i> and <i>Staphylococcus aureus</i>	de Aragão et al. (2019)
<i>Ulva flexuosa</i>	Aqueous filtrate	UV-Vis, FT-IR, FE-SEM, HR-TEM, EDX, AFM, XRD	4.93 - 6.70	Spherical	Reduced the bacterial count (proliferation rate)	Dixit et al. (2018)
<i>Enteromorpha compressa</i>	Aqueous filtrate	UV-Vis, FT-IR, HR-TEM, EDX, XRD	4 -24	Spherical	Effective against different clinical pathogens (both bacteria and fungi)	Ramkumar et al. (2017)

<i>Spirogyra varians</i>	Aqueous filtrate	UV-Vis, FT-IR, SEM, XRD	17.6	Quasi-spheres	Effective against pathogenic microbes	Salari et al. (2016)
<i>Caulerpa racemosa</i>	Aqueous filtrate	UV-Vis, FT-IR, HR-TEM, EDX, XRD, SAED	25	Spherical	Catalytic degradation of methylene blue	Edison et al. (2016)
<i>Acanthophora specifera</i>	Aqueous filtrate	FT-IR, XRD	33 - 81	Cubic	Prevents proliferation of <i>Staphylococcus aureus</i> , <i>Bacillus subtilis</i> , <i>Salmonella</i> spp., <i>Escherichia coli</i> and unicellular fungus <i>Candida albicans</i>	Ibraheem et al. (2016)
<i>Caulerpa racemosa</i>	Aqueous filtrate	UV-Vis, FT-IR, TEM, DLS	5 - 25	Spherical	Effective against human pathogenic microbes (<i>Staphylococcus aureus</i> and <i>Proteus mirabilis</i>)	Kathiraven et al. (2015)
<i>Pithophora oedogonia</i>	Aqueous filtrate	UV-Vis, FT-IR, SEM, EDX, DLS	25 -44	cubical and hexagonal	Inhibit growth of <i>Pseudomonas aeruginosa</i> and <i>Escherichia coli</i>	Sinha et al. (2015)
<i>Sargassum longifolium</i>	Aqueous filtrate	UV-Vis, FT-IR, SEM, TEM, XRD	40 - 85	spherical, truncated and ellipsoidal	Prevents proliferation of pathogenic fungi <i>Aspergillus fumigatus</i> , <i>Candida albicans</i> and <i>Fusarium</i>	Rajeshkumar et al. (2014)
<i>Codium capitatum</i>	Aqueous filtrate	FT-IR, TEM, EDX	3 - 44	Spherical	Effective in the field of biomedicine and agriculture	Kannan et al. (2013)

<i>Ulva fasciata</i>	Ethyl acetate extract	UV-Vis, FT-IR, SEM, EDX, XRD	28 - 41	Spherical	Inhibits proliferation of <i>Xanthomonas campestris</i> pv. <i>malvacearum</i>	Rajesh et al. (2012)
<i>Padina tetrastromatica</i>	Dry algal powder aqueous extracted	UV-Vis, FT-IR, TEM, XRD	14	Spherical	Inhibit the growth of pathogenic and opportune pathogenic bacteria (<i>Bacillus</i> and <i>Pseudomonas</i> ; <i>Bacillus subtilis</i> and <i>Klebsiella planticola</i>)	Rajeshkumar et al. (2012)
<i>Gelidiella acerosa</i>	Aqueous filtrate	UV-Vis, FT-IR, SEM, TEM, XRD	22	Spherical	Inhibit the growth of <i>Humicola insolens</i> , <i>Fusarium dimerum</i> , <i>Mucor indicus</i> and <i>Trichoderma reesei</i>	Vivek et al. (2011)
<i>Sargassum wightii</i>	Aqueous filtrate	UV-Vis, FT-IR, TEM, XRD	5 - 25	Spherical	Effective against <i>Staphylococcus aureus</i> , <i>Bacillus rhizoids</i> , <i>Escherisia coli</i> and <i>Pseudomonas aeruginosa</i>	Govindaraju et al. (2009)

[**Abbreviation used:** UV-Vis = UV-Visible Spectrophotometer; FT-IR = Fourier-Transform Infrared Spectroscopy; SEM = Scanning Electron Microscopy; FE-SEM= Field Emission Scanning Electron Microscopy; TEM= Transmission Electron Microscopy; HR-TEM= High-Resolution Transmission Electron Microscopy; AFM= Atomic Force Microscopy; EDX= Energy Dispersive X-Ray Analysis; XRD= X-Ray Diffraction Analysis; DLS = Dynamic Light Scattering]

Table 6: Fungi mediated synthesis of silver nanoparticles

Fungi Name	Extract Used	Characterization	Size (nm)	Shape	Bioactivity	Reference
<i>Aspergillus sydowii</i>	Fungal filtrate	UV-Vis, TEM, XRD	5 - 15	Spherical	Inhibit the proliferation of fungal pathogens <i>Aspergillus</i> , <i>Fusarium</i> , <i>Candida</i> , and <i>Sporothrix schenckii</i>	Wang et al. (2021)
<i>Bjerkandera</i>	Fungal filtrate	UV-Vis, FT-IR, STEM, HR-TEM, EDX	70 - 90	Spherical	ND	Osorio-Echavarría et al. (2021)
<i>Fusarium scirpi</i>	Fungal filtrate	UV-Vis, FT-IR, SEM, TEM, EDX	2 - 20	Quasi-spherical	Antibacterial activity against <i>E.coli</i>	Rodríguez-Serrano et al. (2020)
<i>Penicillium duclauxii</i>	Fungal filtrate	UV-Vis, , TEM, EDX, XRD	3 - 32	Spherical	Concentration dependent growth control of <i>Bipolaris sorghicola</i>	Almaary et al. (2020)
<i>Penicillium cyclopium</i>	Fungal filtrate	UV-Vis, FT-IR, SEM, TEM	12 - 25	Irregular	ND	Wanarska and Maliszewska (2019)
<i>Fusarium oxysporum</i>	Fungal biomass and PDA media	SEM, TEM, DLS	1 - 50	Spherical	Antibacterial potential	Srivastava et al. (2019)
<i>Trichoderma harzianum</i>	Fungal biomass	UV-Vis, DLS, Zeta Potential	57.20	NM	Controls mycelial growth of <i>Sclerotinia sclerotiorum</i>	Guilger-Casagrande et al. (2019)

<i>Beauveria bassiana</i>	Fungal filtrate	UV-Vis, SEM, TEM, EDX, XRD, ZP	10 - 50	Triangular, circular, hexagonal	Inhibit growth of <i>Escherichia coli</i> , <i>Pseudomonas aeruginosa</i> and <i>Staphylococcus aureus</i>	Tyagi et al. (2019)
<i>Phomopsis liquidambaris</i>	Aqueous extract	UV-Vis, FT-IR, TEM, EDX, ZP	10 - 20	Spherical	Effective against wide range of bacteria	Seetharaman et al. (2018)
<i>Trichoderma longibrachiatum</i>	Fungal biomass	UV-Vis, FT-IR, TEM, DLS	1 - 25	Spherical	Effective against pathogenic fungi	Elamawi et al. (2018)
<i>Duddingtonia flagans</i>	Fungal filtrate	UV-Vis, FT-IR, TEM, XRD, DLS	30 - 409	Spherical	ND	Costa Silva et al. (2017)
<i>Aspergillus versicolor</i>	Fungal biomass	UV-Vis, SEM, TEM	5 - 30	Spherical	Antifungal activity against <i>Sclerotinia sclerotiorum</i> and <i>Botrytis cinerea</i>	Elgorban et al. (2016)
<i>Sclerotinia sclerotiorum</i>	Fungal filtrate	UV-Vis, FT-IR, TEM	10 - 15	Spherical	Effective against <i>Escherichia coli</i> and <i>Staphylococcus aureus</i>	Saxena et al. (2016)
<i>Fusarium oxysporum</i>	Fungal filtrate	UV-Vis, FT-IR, TEM, EDX, DLS	15 - 40	Spherical	Antibacterial and antitumor activity	Husseiny et al. (2015)
<i>Guignardia mangifera</i>	Mycelial free filtrate	UV-Vis, HR-TEM, EDX, XRD, SAED	5 - 30	Spherical	Antibacterial, antifungal and cytotoxic activity	Balakumaran et al. (2015)
<i>Trichoderma harzianum</i>	Mycelia free cell filtrate	UV-Vis, FT-IR, TEM, EDX, XRD, DLS	51.01	Spherical	Effective against <i>Staphylococcus aureus</i> and <i>Klebsiella pneumonia</i>	Ahluwalia et al. (2014)
<i>Neurospora intermedia</i>	Supernatant of PDB media	UV-Vis, FT-IR, SEM, EDX, XRD, DLS	24	NM	Inhibit the growth of <i>Escherichia coli</i>	Hamed et al. (2013)
<i>Fusarium oxysporum</i>	Fungal filtrate	UV-Vis, FT-IR, TEM, SAED	10 - 40	NM	ND	Birla et al. (2013)

<i>Epicoccum nigrum</i>	Suspension of fungal biomass	UV-Vis, TEM, XRD	1 - 22	Spherical	Antifungal activity against pathogenic <i>Candida</i> spp.	Qian et al. (2013)
<i>Rhizoctonia solani</i>	Culture supernatant	UV-Vis, FT-IR, TEM, EDX, XRD	2 - 22	Spherical	ND	Ashrafi et al. (2013)
<i>Aspergillus Niger</i>	Fungal biomass	UV-Vis, TEM	1.7 - 20	Spherical	Antibacterial activity against <i>Bacillus megaterium</i> , <i>Staphylococcus aureus</i> , <i>Proteus vulgaris</i> and <i>Shigella sonnei</i>	Vala and Shah (2012)
<i>Penicillium purpurogenum</i>	Fungal filtrate	UV-Vis, TEM, XRD	8 - 10	Spherical	Displayed antimicrobial effect against <i>Escherichia coli</i> , <i>Pseudomonas aeruginosa</i> and <i>Staphylococcus aureus</i>	Nayak et al. (2011)

[**Abbreviation used:** NM = Not Mentioned; ND = Not Detected; UV-Vis = UV-Visible Spectrophotometer; FT-IR = Fourier-Transform Infrared Spectroscopy; SEM = Scanning Electron Microscopy; FE-SEM = Field Emission Scanning Electron Microscopy; TEM = Transmission Electron Microscopy; HR-TEM = High-Resolution Transmission Electron Microscopy; AFM = Atomic Force Microscopy; EDX = Energy Dispersive X-Ray Analysis; XRD = X-Ray Diffraction Analysis; DLS = Dynamic Light Scattering; ZP = Zeta Potential]

Table 7: Bacteria mediated synthesis of silver nanoparticles

Bacteria Used	Extract used	Characterization	Size (nm)	Shape	Bioactivity	Reference
<i>Lactobacillus plantarum</i>	Bacterial wet biomass	UV-Vis, FT-IR, SEM, HR-TEM, EDX, DLS	4.7 - 24.3	Spherical	Antibacterial and antioxidant activity	Yusof et al. (2020)
<i>Bacillus siamensis</i>	Bacterial culture filtrate	UV-Vis, FT-IR, SEM, TEM, EDX, XRD	25 - 50	Spherical	Protecting rice plants from bacterial leaf blight and brown stripe diseases	Ibrahim et al. (2019)
<i>Escherichia coli</i>	Bacterial culture filtrate	SEM, TEM, EDX	10.6	NM	Antimicrobial activity	Baltazar-Encarnación et al. (2019)
<i>Bacillus brevis</i>	Bacterial culture filtrate	UV-Vis, FT-IR, SEM, AFM	22 - 60	Spherical	Effective against pathogenic bacteria <i>Staphylococcus aureus</i> and <i>Salmonella typhi</i>	Saravanan et al. (2018)
<i>Leuconostoc lactis</i>	Partially purified exopolysaccharide	UV-Vis, FT-IR, SEM, TEM, AFM, XRD	30 - 200	Spherical	Biodegradation of harmful textile dyes	Saravanan et al. (2017)
<i>Gordonia amicalis</i>	Bacterial cell free suspension	UV-Vis, FT-IR, TEM, XRD	5 - 25	Cubic	Free radical scavenging activity	Sowani et al. (2016)

<i>Ochrobactrum rhizosphaerae</i>	Bacterial cell free suspension	UV-Vis, FT-IR, TEM, EDX, DLS	2 - 20	Spherical	Effective against cholera disease	Gahlawat et al. (2016)
<i>Sinomonas mesophila</i>	Bacterial cell free suspension	UV-Vis, FT-IR, TEM	4 - 50	Spherical	Effective against multi drug resistant <i>Staphylococcus aureus</i>	Manikprabhu et al. (2016)
<i>Bacillus</i>	Bacterial cell free suspension	UV-Vis, SEM, TEM, EDX	7 - 31	Spherical	Effective against <i>Escherichia coli</i> and <i>Salmonella typhi</i>	Deljou and Goudarzi (2016)
<i>Bacillus</i>	Bacterial cell free suspension	UV-Vis, TEM	42 - 92	NM	ND	Das et al. (2014)
<i>Acinetobacter calcoaceticus</i>	Bacterial cell free suspension	UV-Vis, TEM, HR-TEM, EDX	8 - 12	Spherical	Effective against some drug-resistant bacterial strains	Chopade et al. (2013)
<i>Enterobacter aerogenes</i>	Bacterial cell free suspension	UV-Vis, SEM, TEM, EDX	25 - 35	Spherical	ND	Karthik and Radha (2012)
<i>Morganella morganii</i>	Culture suspension	UV-Vis, TEM, XRD, SAED	10 - 50	Quasispherical	ND	Parikh et al. (2011)
<i>Geobacillus stearothermophilus</i>	Bacterial cell free suspension	UV-Vis, FT-IR, TEM, XRD	5 - 35	Spherical	ND	Mohammed Fayaz et al. (2011)

<i>Streptomyces hygroscopicus</i>	Bacterial cell free suspension	UV-Vis, FE-SEM, TEM, AFM, XRD	20 - 30	Spherical	Inhibit the growth of <i>Bacillus subtilis</i> , <i>Enterococcus faecalis</i> , <i>Escherichia coli</i> and <i>Salmonella typhimurium</i>	Sadhasivam et al. (2010)
-----------------------------------	--------------------------------	-------------------------------	---------	-----------	---	--------------------------

[**Abbreviation used:** NM = Not Mentioned; ND = Not Detected; UV-Vis = UV-Visible Spectrophotometer; FT-IR = Fourier-Transform Infrared Spectroscopy; SEM = Scanning Electron Microscopy; FE-SEM = Field Emission Scanning Electron Microscopy; TEM = Transmission Electron Microscopy; HR-TEM= High-Resolution Transmission Electron Microscopy; AFM = Atomic Force Microscopy; EDX = Energy Dispersive X-Ray Analysis; XRD = X-Ray Diffraction Analysis; DLS = Dynamic Light Scattering]

2.2.5.3.4. Synthesis of silver nanoparticle by plants extract

Different plant parts *viz.* root, stem, bark, leaf, bud, fruit, latex, and others are used for biogenic synthesis of silver nanoparticles (Ahmed and Mustafa 2020). The plant extract acts as a pool of different phytochemicals *viz.* phenol, flavones, terpenoids, aldehydes, ketones, carboxylic acids, enzymes, amides, and many more which donates electron for reduction of metallic ion to nano form (Masum et al. 2019). Plant extract mediated green synthesis bears additional advantage over physical and chemical methods of synthesis because of their simple, rapid, environment friendly, non-toxic, and cost effective nature (Chanel et al. 2017). Besides this, plant material used for nano synthesis should be easily available under natural condition (Chung et al. 2016). It has also been reported that nanoparticles synthesized by green technology bears more bioactivity than synthesized through chemical methods (Choudhury et al. 2016). It has also been reported that plant extract mediated synthesis of silver nanoparticles displayed potential antioxidant (Ansar et al. 2020) and antimicrobial activities (Salayová et al. 2021; Okafor et al. 2013). Different plant extracts that are used for the biosynthesis of silver nanoparticles are enlisted in Table 8.

2.2.6. Characterization and validation of green synthesized silver nanoparticles

The techniques that are generally adopted for nano characterization are UV-Visible spectroscopy, Fourier-transform infrared spectroscopy (FTIR), dynamic light scattering (DLS), scanning electron microscope (SEM), transmission electron microscopy (TEM), X-ray diffraction (XRD) and atomic force microscopy (AFM).

2.2.6.1. UV-Visible spectroscopy

UV-Visible spectrophotometer works following Beer Lambert law, in which when light falls on the sample, the amount of light absorbed is directly proportional to the path length and concentration of the sample (Abbas 2019). The compound that is formed after reaction between silver nitrate with plant extract was generally confirmed by UV-Visible spectroscopy in the range of 350 – 700 nm (Sumi Maria et al. 2014). Appearance of spectral peak in the wavelength range of 400 – 500 nm confirms the formation of silver nanoparticles (Sastry et al. 1997). The appearance of surface plasmon resonance (SPR) peak depends upon dielectric environment

along with size, shape and composition of the nanoparticles (Sahu et al. 2021). Prasad and Elumalia (2011) on synthesizing nanosilver using extract of *Moringa oleifera* displayed absorption peak in the range of 430 – 440 nm. Bagherzade et al. (2016) confirms the formation of silver nanoparticle using aqueous extract of *Crocus sativus* by observing appearance of Surface Plasmon Resonance (SPR) at 450 nm. Nanosilver formed using aqueous extract of *Otostegia persica* shows absorption peak at 420 nm (Sharifi-Rad et al. 2021). Kumar et al. (2014) observed absorption peak at 430 nm when green synthesis was done using leaf extract of *Alternanthera dentate*. Nano Silver prepared using extract of blackberry fruit shows absorption peak at 435 nm (Kumar et al. 2015).

2.2.6.2. Fourier-transform infrared spectroscopy (FT-IR)

FT-IR analysis was done to determine the functional groups involved in nanosilver formation. FT-IR spectroscopy provide the detection of small changes in absorbance in the order of 10^{-3} by which one could understand the small changes in absorption bands of active residue from the total absorption of entire molecule (Kim and Barry 2001). FT-IR spectra help in determining the nature of bonding and structural characteristics of conjugate complexes (Huq et al. 2020). In FT-IR analysis, when infrared light is projected stretching, contraction and bending of bonds takes place, due to which absorption of infrared radiation of specific wavelength takes place by the functional groups present in the molecules (Kumar and Yadav 2008). FTIR spectroscopy is widely used to search the involvement of biomolecules in the synthesis of nanoparticles, which is very demanding in academic and industrial areas (Lin et al. 2014). FTIR is very important to the study of nano-scaled materials, provides confirmation of functional molecules covalently attached onto silver, carbon and gold nanoparticles (Gurunathan et al. 2014). The advance level of FT-IR method is attenuated total reflection (ATR)-FTIR spectroscopy. ATR-FTIR helps in understand the chemical properties on the surface of the polymer and side by side sample preparation; for this, method is easier than conventional FT-IR (Hind et al. 2001).

Table 8: Plants mediated synthesis of silver nanoparticles

Plant Name	Extract Used	Extraction solvent	Characterization	Size (nm)	Shape	Bioactivity	Reference
<i>Tropaeolum majus</i>	Dried leaf	Aqueous	UV-Vis, FT-IR, AFM	25	Crystalline	Anti-microbial activity against <i>Klebsiella pneumonia</i> , <i>Staphylococcus aureus</i> and <i>Bacillus subtilis</i>	Bawazeer et al. (2021)
<i>Jasminum officinal</i>	Dried leaf	Aqueous	UV-Vis, FT-IR, TEM, HR-TEM, XRD, DLS	9.22	Spherical	Exhibits cytotoxic activity against 5637 and MCF-7 cell lines	El-Hawary et al. (2020)
<i>Clinacanthus nutans</i>	Dried leaf	Aqueous	UV-Vis, FT-IR, SEM, TEM, EDS, XRD, DLS, ZP	114.7	Spherical	ND	Mat Yusuf et al. (2020)
<i>Clinacanthus nutans</i>	Dried Stem	Aqueous	UV-Vis, FT-IR, SEM, TEM, EDS, XRD, DLS, ZP	129.9	Spherical	ND	Mat Yusuf et al. (2020)
<i>Muntingia calabura</i>	Dried leaf	Aqueous	UV-Vis, FT-IR, SEM, TEM, EDS	30 - 60	Spherical	Antimicrobial activity against <i>Escherichia coli</i> and <i>Bacillus cereus</i>	Ahmad et al. (2020)
<i>Calligonum comosum</i>	Root	Aqueous	UV-Vis, FT-IR, SEM, TEM, ZP	183.2	Spherical	Exhibits apoptotic potential against HepG2, LoVo and MDA-MB 231- cell	Algebaly et al. (2019)
<i>Solanum mammosum</i>	Dried Fruit	Aqueous	UV-Vis, SEM, TEM, EDX, XRD, DLS	10 - 14	Spherical	Larvicidal activity against <i>Aedes aegypti</i>	Pilaquinga et al. (2019)

<i>Phyllanthus emblica</i>	Fresh Fruit	Aqueous	UV-Vis, FT-IR, SEM, TEM, HR-TEM, EDX, XRD, SAED	19.8 - 92.8	Spherical	Inhibits proliferation of <i>Acidovorax oryzae</i>	Masum et al. (2019)
<i>Ipomoea Pes-Caprae</i>	Stem	Aqueous	UV-Vis, FT-IR, TEM, XRD, DLS	116	Spherical	Effective against pathogenic microbes (<i>Escherichia coli</i> , <i>Pseudomonas aeruginosa</i>)	Veeramani et al. (2018)
<i>Punica granatum</i>	Dried leaf	Aqueous	UV-Vis, FT-IR, TEM, XRD, EDAX	88 - 120	Spherical, rhomboid and cubical	ND	Kumar et al. (2018)
<i>Carica papaya</i>	Dried epidermal peel	Aqueous	UV-Vis, SEM, TEM, XRD, SAED	15 - 20	Spherical	Antibacterial activities against <i>Escherichia coli</i> and <i>Staphylococcus aureus</i>	Balavijayalakshmi and Ramalakshmi (2017)
<i>Zingiber officinale</i>	Dried rhizomes	Ethanol	UV-Vis, FT-IR, TEM, XRD	10	Spherical	Antimicrobial activity against <i>Vibrio anguillarum</i> , <i>Vibrio alginolyticus</i> , <i>Aeromonas punctata</i> , <i>Vibrio parahaemolyticus</i> , <i>Vibrio splendidus</i> and <i>Vibrio harveyi</i>	Nan et al. (2017)
<i>Azadirachta indica</i>	Leaf	Aqueous	UV-Vis, FT-IR, TEM, DLS	34	Spherical	Effective against gram positive (<i>Staphylococcus aureus</i>) and gram negative (<i>Escherichia coli</i>) bacteria	Ahmed et al. (2016)
<i>Couroupita guianensis</i>	Leaf	Aqueous	UV-Vis, FT-IR, XRD, TEM	10 - 45	Cubic	Dose dependent larvicidal effect	Vimala et al.

					crystalline	against <i>Aedes aegypti</i>	(2015)
<i>Couroupita guianensis</i>	Fruit	Aqueous	UV-Vis, FT-IR, XRD, TEM	5 -15	Cubic crystalline	Dose dependent larvicidal effect against <i>Aedes aegypti</i>	Vimala et al. (2015)
<i>Ziziphora tenuior</i>	Dried leaf	Methanol	UV-Vis, FT-IR, SEM, TEM, XRD	8 - 40	Spherical	ND	Sadeghi and Gholamhoseinpoor (2015)
<i>Tephrosia purpurea</i>	Fresh Leaf	Aqueous	UV-Vis, FT-IR, FE-SEM, TEM, XRD, EDX	16	Spherical	Antipathogenic activity against <i>Pseudomonas</i> and <i>Penicillium</i>	Ajitha et al. (2014)
<i>Eucalyptus leucoxydon</i>	Leaf	Aqueous	UV-Vis, SEM, TEM, XRD	50	Spherical	Potential antioxidant activity	Rahimi-Nasrabadi et al. (2014)
<i>Myrmecodia pendan</i>	Entire Plant	Aqueous	UV-Vis, FT-IR, SEM, TEM, XRD	10 - 20	Cubic crystalline	ND	Zuas et al. (2014)
<i>Withania somnifera</i>	Dried leaf	Aqueous	UV-Vis, FT-IR, TEM, EDS, XRD, ZP, NTA	5 - 30	Spherical	Antipathogenic activity against <i>Staphylococcus aureus</i> , <i>Escherchia coli</i> , <i>Candida</i> <i>albicans</i> , <i>Aspergillus niger</i> and <i>Aspergillus flavus</i>	Raut et al. (2014)
<i>Epiphyllum Oxypetalum</i>	Fresh Fruit	Aqueous	UV-Vis, FT-IR, ZP	86	Spherical	Antimicrobial activity against <i>Propionibacterium acne</i> , <i>Pseudomonas</i> <i>aeruginosa</i> and <i>Klebsiella</i> <i>pneumoniae</i>	Paralikaar (2014)
<i>Cocos nucifera</i>	Coconut-	Aqueous	UV-Vis, SEM,TEM, EDX, XRD	23	Spherical	Anti-larvicidal activity against	Roopan et al.

	coir						<i>Anopheles stephensi</i>	(2013)
<i>Lxora coccinea</i>	Leaf	Aqueous	UV-Vis, FT-IR, FE-SEM, XRD	13 - 57	Spherical	ND		Karuppiah and Rajmohan (2013)
<i>Elaeagnus indica</i>	Leaf powder	Aqueous	UV-Vis, FT-IR, TEM, DLS	30	Spherical		Effective against bacterial (<i>Escherichia coli</i> , <i>Pseudomonas putida</i> , <i>Bacillus subtilis</i> and <i>Staphylococcus aureus</i>) and fungal (<i>Aspergillus flavus</i> and <i>Fusarium oxysporium</i>) pathogens	Natarajan et al. (2013)
<i>Azadirchata indica</i>	Leaf	Aqueous	UV-Vis, TEM, XRD	15 - 20	Spherical		Application towards heavy metal ion sensor like copper	Kirubaharan et al. (2012)
<i>Morinda citifolia</i>	Leaf	Aqueous	UV-Vis, FT-IR, SEM, HR-TEM, EDX, SAED	10 - 60	Spherical		Effective against human pathogenic microbes (<i>Escherichia coli</i> , <i>Pseudomonas aeruginosa</i> , <i>Klebsiella pneumoniae</i> , <i>Enterobacter aerogenes</i> , <i>Bacillus cereus</i> and <i>Enterococci</i> sp.)	Satishkumar et al. (2012)
<i>Crossandra infundibuliformis</i>	Leaf	Aqueous	UV-Vis, FT-IR, FE-SEM-EDAX, XRD	38	Cubic crystalline	ND		Kaviya et al. (2012)
<i>Tribulus terrestris</i>	Fruit	Aqueous	UV-Vis, FT-IR, TEM, AFM, XRD	16 - 28	Spherical		Effective against <i>Streptococcus pyogens</i> , <i>Pseudomonas aeruginosa</i> , <i>Escherichia coli</i> , <i>Bacillus subtilis</i> and	Gopinath et al. (2012)

							<i>Staphylococcus aureus</i>	
<i>Ocimum tenuiflorum</i>	Leaf	Aqueous	UV-Vis, TEM, SAED, DLS, ZP	25 - 40	Spherical	Effective against different bacterial strains of <i>Escherichia coli</i> , <i>Corney bacterium</i> , <i>Bacillus substilus</i>	Patil et al. (2012)	
<i>Catharanthus roseus</i>	Leaf	Aqueous	UV-Vis, SEM, XRD, EDX	48 - 67	Cubic crystalline	ND	Mukunthan et al. (2011)	
<i>Eclipta prostrate</i>	Leaf	Aqueous	UV-Vis, FT-IR, SEM, TEM, XRD	35 - 60	Cubic crystalline	Controls proliferation of <i>Culex tritaeniorhynchus</i> and <i>Anopheles subpictus</i>	Rajakumar and Abdul Rahuman (2011)	
<i>Lonicera japonica</i>	Leaf	Aqueous	UV-Vis, FT-IR, TEM, EDX, AFM, ZP	36 - 72	Spherical	ND	Kumar and Yadav. (2011)	
<i>Nelumbo nucifera</i>	Dried leaf	Aqueous	UV-Vis, FT-IR, SEM, TEM, XRD	25 - 80	Spherical, triangle, truncated triangles, and decahedral	Mosquito larvicidal activity	Santoshkumar et al. (2011)	
<i>Citrus limon</i>	Fruit	Aqueous	UV-Vis, FT-IR, TEM, AFM, XRD	50	Spherical and spheroidal	ND	Prathna et al. (2011)	
<i>Fissidens minutus</i>	Thallus	Aqueous and 70%	UV-Vis, SEM, EDS	NM	Spherical and	Antimicrobial activity against <i>Escherichia coli</i> , <i>Bacillus cereus</i> ,	Srivastava et al. (2011)	

		ethanol			spheroidal	<i>Klebsiella pneumoniae</i> and <i>Pseudomonas aeruginosa</i>	
<i>Cycas</i>	Leaf	Aqueous-ethanolic	UV-Vis, TEM, XRD	2 - 6	Spherical and spheroidal	ND	Jha and Prasad. (2010)
<i>Acalypha indica</i>	Leaf	Aqueous	UV-Vis, SEM, TEM, EDS, XRD	20 - 30	Spherical	Effective against water borne pathogens (<i>Escherichia coli</i> and <i>Vibrio cholera</i>)	Krishnaraj et al. (2010)
<i>Piper nigrum</i>	Seed	Aqueous	UV-Vis, TEM, XRD	20 - 50	Spherical	ND	Shukla et al. (2010)
<i>Tanaetum vulgare</i>	Fruit	Aqueous	UV-Vis, FT-IR, TEM, XRD, EDAX	10 - 40	Hexagonal	ND	Dubey et al. (2010)

[**Abbreviation used:** NM = Not Mentioned; ND = Not Detected; UV-Vis = UV-Visible Spectrophotometer; FT-IR = Fourier-Transform Infrared Spectroscopy; SEM = Scanning Electron Microscopy; FE-SEM = Field Emission Scanning Electron Microscopy; TEM = Transmission Electron Microscopy; HR-TEM = High-Resolution Transmission Electron Microscopy; AFM = Atomic Force Microscopy; EDX = Energy Dispersive X-Ray Analysis; XRD = X-Ray Diffraction Analysis; DLS = Dynamic Light Scattering; ZP = Zeta Potential]

2.2.6.3. X-ray diffraction (XRD)

The device that is widely used for determining the crystalline structure and size of the synthesized nanoparticles is X-ray diffraction (Garcia et al. 2020). Nanosilver solution was dried at 60°C before characterizing through XRD (Verma and Mahata 2016). The crystalline nature of silver nanoparticles was determined using XRD analysis using the dry powder of nanoparticle (Yu et al. 2019). There is a strong correlation between the size of nanoparticle that is obtained by TEM and XRD, it has been found that size of nanoparticles that is obtained through XRD generally remains same or slightly smaller than that of the size determined through TEM analysis (Ungár et al. 2005).

2.2.6.4. Dynamic light scattering (DLS)

DLS study was done to determine the size range of nano particles in suspension (Kim et al. 2019). Bhattacharjee (2016) stated that DLS study of prepared nanosilver was done for determining the size distribution, as well as for determining surface charge through analysing zeta potential. Patil et al. (2012) stated that the negative value of zeta potential indicates stability of nanoparticles. DLS measures hydrodynamic radiuses of the synthesized nanoparticles and takes into consideration associated capping and reducing agents while measuring size and thus DLS size is greater than TEM size of nanoparticles (Kaasalainen et al. 2017).

2.2.6.5. Scanning electron microscopy (SEM) and energy dispersive X-ray (EDX)

High resolution microscopes have wide applicability in the field of nanoscience and nanotechnology as it helps in studying ultra-structure of nanomaterials (Pawley 1997). Scanning electron microscopy (SEM) is a method that scans the surface morphology of nanoparticles and thereby predicting their shape and particle distribution pattern (Vladára and Hodoroba 2020). EDX provides the elemental profile of biosynthesized nanoparticle (Femi-Adepoju et al. 2019).

There is a limitation of SEM analysis, as it cannot detect the internal structure of a particle, but it can provide important information about the purity of the sample and the degree of aggregation of the particles in that sample and lastly modern high-

resolution SEM can detect the surface morphology of nanoparticles below 10 nm (Rydz et al. 2019; Mourdikoudis et al. 2018).

2.2.6.6. Transmission electron microscopy (TEM)

Transmission electron microscopy (TEM) is very important, commonly used technique for quantitative characterization of nanoparticles in respect to particle size and range of size distribution (Santiago et al. 2018). Beside this TEM also predicts morphology of the nanoparticles (Joshi and Bhattacharyya 2008). Ahmed et al. (2016) reported that TEM analysis was performed for determining the particle size, shape and surface morphology. Rice et al. (2013) stated that microscopy is the only method for measuring the individual particle size. TEM analysis of synthesized nanoparticle using extract of *Brillantaisia patula*, *Crossopteryx febrifuga* and *Senna siamea* displayed spherical shaped nanoparticles with average size dimension of 45, 115 and 47 nm respectively (Kambale et al. 2020). Bagherzade et al. (2016) reported that shape and size of the silver nanoparticle formed using aqueous extract of saffron wastage was spherical and 15 nm respectively. Kumar et al. (2014) reported spherical shaped nanosilver when green synthesis was done with leaf extract of *Alternanthera dentate*.

2.2.7. Factors affecting nanoparticles formation

Formation of bioactive nanoparticles depends upon number of factors including temperature, pH, concentration of reactants and reaction time.

2.2.7.1. Effect of temperature on silver nanoparticle synthesis

Increase in temperature during green synthesis gradually leads to decrease in SPR peak and thereby decrease in size of formed nanoparticles takes place (Ibrahim 2015). Kumar et al. (2014) reported that with increase in temperature blue shift (decrease in wavelength) takes place in surface plasmon resonance band. Khatoun et al. (2017) reported that with increase in temperature, reaction rate increases due to which reduction of silver ions occurs at lesser time, leading to the formation of smaller size particles. Rao and Tang (2017) reported that high temperature is favourable for biosynthesis of nanosilver as it provides greater concentration of silver nanoparticles along with small and uniform size particles.

2.2.7.2. Effect of pH on silver nanoparticle synthesis

pH alters the surface charge of nanoparticles, so it plays an important role in reduction of silver ion, as well as in determining shape, size and stability of nanoparticles (Khatoon et al. 2017). Dubey et al. (2010) while working with tansy fruit for nanoparticle synthesis observed low zeta potential at acidic pH and high at alkaline pH. Jayapriya and Lalitha (2013) reported that in comparison to acidic pH, at basic pH formation of nanosilver takes place more rapidly. Alqadi et al. (2014) reported inverse relationship between size of the nanoparticles and pH of the reaction media because when pH of the reaction mixture increases the size of the silver nanoparticles decreases and vice versa. Maria et al. (2015) observed through spectral analysis that at low pH (pH 3), no characteristic SPR peak was formed, while at pH 7 characteristic SPR peak was noted and at pH 11 a very well peak is developed, indicating higher or alkaline pH is much suitable for the synthesis of silver nanoparticles.

2.2.7.3. Effect of concentration on silver nanoparticle synthesis

Shankar et al. (2017) reported that with increase in concentration of silver nitrate, formation of nanosilver increases which was confirmed by increase in wavelength of plasmon peak. Jayapriya and Lalitha (2013) used different concentration of silver nitrate (1ml, 2ml, 3ml, 4ml and 5ml) with a particular concentration of plant extract (1ml) for the synthesis of silver nanoparticles and they observed that best formation of nanosilver particles occurred when 5ml silver nitrate solution was mixed with 1ml plant extract at room temperature. Intensity of the SPR peak increases in concentration of silver nitrate solution from 1 to 10 mM and in case of 10 mM silver nitrate concentration the peak appeared at 418 nm (Zaki et al. 2011). Dubey et al. (2010) also reported similar phenomenon i.e., increase in peak intensity takes place with increase in concentration of salt.

2.2.7.4. Effect of reaction time on silver nanoparticle synthesis

Krishnaraj et al. (2010) reported that greater the reaction time between silver nitrate with plant extract more is the concentration of synthesized nanoparticle. Rao and Tang (2017) reported that increase in biosynthesis of silver nanoparticles over time can be monitored using UV-Vis spectrophotometer, as the intensity of peak

gradually increases over time. Shankar et al. (2017) also reported that formation of nanosilver increases with increase in time of reaction, as revealed by increase in intensity of plasmon peak. Logeswari et al. (2015) observed that the colour of the reaction mixture changes gradually from light yellow to dark yellow to dark brown along with the time which indicates nano formation. Ahmed et al. (2016) recorded the spectral peak of synthesized nanoparticles at different time intervals viz. 1 hr, 2 hr, 3 hr, 4 hr, 18 hr and 24 hr and observed that the intensity of absorption peaks, as well as intensity of colour of the reaction mixture increased with increase in duration of incubation period.

2.2.8. Bioactive potentiality assessment of green synthesized silver nanoparticles

2.2.8.1. Antioxidant activity of green synthesized silver nanoparticles

Otunola et al. (2017) used 1, 1-diphenyl-2-picrylhydrazyl (DPPH) and 2, 2-Azino-bis (3-ethylbenzthiazoline-6-sulfonic acid) (ABTS) assays to examine the antioxidant activities of plant species and silver nanoparticles. Silver nanoparticles which were synthesized using leaf extracts of *Leptadenia reticulata* gave the highest record of free radical scavenging activity of 64.81% at a concentration of 500 µg/ml (Swamy et al. 2015). Plant extracts is a pool of large number of phenolic compounds which displayed high antioxidant properties and reduction activity, and this potentiality was used synthesis of silver nanoparticles (Quaresma et al. 2009). Mohamed et al. (2013) observed that mixture of plant extract and silver nitrate i.e., silver nanoparticles showed greater scavenging activity than the plant extract alone. Biogenic silver nanoparticles synthesized using extract of *Ananas comosus* (Das et al. 2019) and *Erythrina suberosa* (Mohanta et al. 2017) displayed potent antioxidant activity against generated oxidative stress.

2.2.8.2. Efficiency of green synthesized silver nanoparticles against microorganisms

Antimicrobial activity was performed to determine the minimum concentration at which a particular compound is effective against concerned microorganism. Nanoparticles prepared using copper, zinc, aluminium, titanium and silver displayed potential biocidal properties (Toker et al. 2013). Monores et al. (2005) stated that antimicrobial activity increases if the size of the formed nanoparticles is less than

100 nm. Among all the reported metal ions used for synthesis of nanoparticles, nanoparticles synthesized with silver ion showed best result because of their large surface area which is useful to make surface contact with microorganisms (Rai et al. 2009). The antimicrobial activity of nanosilver depends upon its property to release Ag^+ which interacts with target cell in ionic form (Dong et al. 2019). Monores et al. (2005) reported that silver nanoparticles attack cell division and respiratory chain causing death of the microbes. Gao et al. (2014) reported that due to the presence of antimicrobial activity in silver nanoparticles, it is widely used in the field of medicine, food preservation, cosmetics, and many other industries. Silver has a tendency to act as an intercalating agent and thereby stopping the process of replication in microorganisms (Mikhailova 2020). Beside these, amino acids, mainly cysteine has a tendency to bind with silver ion and thereby disturbing the process of protein synthesis that are involved in major metabolic pathways, due to which microorganisms fails to perform vital functions leading to their death (Percival et al. 2005). Stoimenov et al. (2002) reported that nanosilver was effective against both gram positive and gram negative bacteria. Green synthesized silver nanoparticle using neem extract was found to be effective against both gram positive (*Staphylococcus aureus*) and gram negative (*Escherichia coli*) bacteria (Ahmed et al. 2016). Ali et al. (2016) observed that silver nanoparticles prepared using apple extract at a concentration of 1000 $\mu\text{g/ml}$, 500 $\mu\text{g/ml}$ and 125 $\mu\text{g/ml}$ was effective against *Staphylococcus aureus*, *Pseudomonas aeruginosa* and *Escherichia coli* respectively. Bagherzade et al. (2016) reported that biosynthesized silver nanoparticles showed better and prominent growth inhibition against test organisms in comparison to purchased silver nanoparticles. Kumar et al. (2014) reported that nanosilver at 50 $\mu\text{g/ml}$ was effective against *Aeromonas hydrophila*, *Flavobacterium branchiophilum* and *Pseudomonas fluorescens*.

2.2.9. Application of green synthesized silver nanoparticles

Silver nanoparticles green synthesized using phyto extracts has wide field of application in medical, industrial, and biological field, described below:

2.2.9.1. Application of silver nanoparticles in enhancing post-harvest shelf life of horticultural crops

Halevy and Mayak (1974) stated that at post-harvest stage, horticulture industry faces major problem due to the appearance of early senescence and the prime cause for this in cut flowers was microbial contamination, inhibition of water uptake due to vascular system blockage, excessive water loss and enhancement in ethylene production. Combinational treatment of nanosilver (1 mgdm^{-3}) and sucrose (2%) prevents petal senescence and thereby extends post-harvest life of 'Cut Lisianthus' (Skutnik et al. 2021). Nanosilver solution has been reported to act as a novel biocide, as it prevents senescence and extends vase life of *Cosmos bipinnatus* (Skutnik et al. 2020). Combination of sucrose (4%) along 2 or 4 ppm PbSNPs (Piper betle silver nanoparticles) in vase solution extends the post-harvest shelf life of cut spike of *Gladiolus* (Maity et al. 2019). Similarly, silver nanoparticles at 35 ppm concentration were reported to enhance post-harvest shelf life of *Lilium orientalis* (Nemati et al. 2014). Liu et al. (2009) reported that nanosilver pulse treatment enhances the vase life of *Gerbera* by inhibiting microbial growth and thereby preventing xylem blockage. Beni et al. (2013) reported that humic acid and nanosilver treatment enhances fresh weight and water conduction capability in cut tuberose. Byczyńska (2017) reported that among the used concentrations of nanosilver (10, 20, 40 mg/lit), 10 mg/lit concentration provide best result in postharvest shelf life extension of cut tulip flower. Alimoradi et al. (2013) found that nanosilver treatment at post-harvest stage extends vase life by retaining chlorophyll content and by preventing wilting. Hatima et al. (2013) reported that enhancement of vase life of red rose took place if combinational pulse treatment of 5% sucrose and 50 mg/lit silver nanoparticle was given, as it enhances water uptake capacity and prevents loss of fresh weight. Liua et al. (2012) reported vase life extension of *Acacia holosericea* by pulse treatment of neutral and acidic nanosilver.

2.2.9.2. Application of silver nanoparticles in food packaged

Increasing day to day demand of ready-to-eat and cook foods has drawn a major concern of food industry towards supply of high quality and contamination free preserved foods. Bumbudsanpharoke and Ko (2015) reported the continuously increasing demand of nano based material in food packaging industry. Due to the presence of anti-viral, antimicrobial and anti-fungi activity silver nanoparticles amalgamated with edible polymers in active packaging of food (Carbone et al. 2016). Martinez-Abad et al. (2012) reported that application of silver nanoparticles

in packaging industry enhances the shelf life of packaged food and thereby lowers the risk of pathogen contamination. Becaro et al. (2016) reported enhanced shelf life of sliced carrot by reducing microbial contamination when treated with low concentration of nanosilver before packaging. Zandi et al. (2013) reported retention of ascorbic acid content in strawberry (which generally reduces with storage time) when packaged in nanosilver based polypropylene and polyethylene containers. Shah et al. (2015) observed that shelf life of silver nanoparticle coated mandarin stored at 4°C enhances by 120 days.

2.2.9.3. Application of silver nanoparticles in medicine industry

From the very early age silver has been used in the treatment of various diseases including burns and wound infections (Lansdown 2006; Muangman et al. 2006; Dowsett 2004). Silver nanoparticles bear large scale of biomedical application including drug delivery, medical device coating, diagnosis and treatment (Ge et al. 2014). Application of silver nanoparticles is increasing in medical industries because of their active antimicrobial and antifungal properties (Shrivastava 2007; Sanpui et al. 2008). Various clinically used medical products are developed using silver nanoparticles (Burduşel et al. 2018). Silver nanoparticles are used in the treatment of external infection like wound healing dressing materials (Atiyeh et al. 2007; Hermans 2006; Qin 2005). Several commercial products such as gauze, film coating, and bandage are now available which actually remain coated with silver salt or silver nanoparticles (Pirnay et al. 2003; Gupta et al. 2001). Silver nanoparticles has been reported detect and destroy cancerous cells (Patra et al. 2014) using laser therapy (Ge et al. 2014). Jeremiah et al. (2020) reported effectiveness of silver nanoparticles on SARS-CoV-2 as potent microbicides against. Silver nanoparticles have been reported to be used as surface disinfectants against SARS-CoV-2 (COVID-19) (Talebian et al. 2020). Beside this silver nanocluster-silica composite sputtered coating on FFP3 mask has been reported to be effective against Coronavirus SARS-CoV-2 (Balagna et al. 2020).

2.2.9.4. Application of silver nanoparticles in cosmetics industry

The use of silver nanoparticle in cosmetic industry is being practiced for more than a decade. Due to their nano size dimension, silver nanoparticles can penetrate into the skin and other organs easily (Raj and Jose 2012). Nanosilver mediated products are

used in numerous cosmetic articles including hair care products, moisturizer, makeup and sunscreen (Gajbhiye and Sakharwade 2016). Silver nanoparticles can reduce some skin diseases and there were no drastic side effects of silver nanoparticles application was recorded on human health (Campbell et al. 2012). Silver nanoparticles at 0.002 – 0.02 ppm concentration in cosmetic products can easily penetrate human skin without any toxic effect (Kokura et al. 2010).

2.3. Biochemical, enzymological and histological perspective of post-harvest preservation

From biological point of view preservation is a process of maintaining original integrity of biological samples. In agricultural and horticultural science for fulfilling global requirement, different economically important crops (bearing food or medicinal value) and flowering twigs or cuttings are often required to be preserved at post-harvest stage (Aidoo 1993). Preservation can be divided into different categories viz. fresh preservation and dry preservation, chilling, freezing, and pasteurization (Amit et al. 2017). Food sources that are consumed in fresh form like leafy vegetables and fruits face a short post-harvest shelf life (De Corato 2020). Mahajan et al. (2014) stated that the metabolic system of plants remains active after harvest which gradually undergoes senescence and ripening with time, and this process of gradual degradation must be controlled to prolong postharvest shelf life. For maintaining the quality during post-harvest stage, different preservatives have been recommended (Damunupola and Joyce 2008; Ichimura et al. 2016). Most of the preservative solutions usually contain a carbohydrate energy source and a biocide that inhibits bacterial proliferation within the preservative solution (Redman et al. 2002). During post-harvest preservation, changes in biochemical content and enzyme activity decide the ultimate fate of the preserved vegetables, fruits, leaves and flowers. Kazemi et al. (2011) on studying preservation of cut *Eustoma grandiflorum* stated that accumulation of free proline above threshold level is a general indicator of senescence. Skutnik et al. (2021) on studying vase life of cut *Lisianthus* observed that accumulated free proline level gets reduced by several folds when nanosilver was used as preservative than control set (normal water). Another important primary metabolite was chlorophyll whose content retention during post harvest stage indicates health status of leaves. Rajinder et al. (1980) reported that peroxidation of membrane lipid chloroplast was the another reason for chlorophyll

content degradation during leaf senescence. Ferrante et al. (2002) while studying effect of hormones on vase life of *Eucalyptus parvifolia*, stated that cytokinin prevents chlorophyll degradation and thereby prolonging shelf life. Plants store carbohydrate as reserve food material and it serves as energy source during induction of stress. In vase solution, degradation of carbohydrate source mainly sucrose, affects the respiration potentiality of plants which ultimately results in senescence (Ferrante and Reid 2006; Reid 1991).

During the course of preservation, excessive accumulation of superoxide, hydrogen peroxide and other ROS related molecules inside tissue system leads to the generation of oxidative stress. Ishida et al. (2014) reported that chloroplast lumen was the major site for ROS production. Generated ROS is capable in causing oxidative injury to primary metabolites viz. carbohydrates, lipids, proteins and nucleic acids, while generation and accumulation of ROS above threshold level causes cellular death (Ismail et al. 2015; Anjum et al. 2015). To overcome the toxic effect of ROS and to prolong the shelf life, plants activate certain defensive activities. Antioxidant enzymes like superoxide dismutase, catalase, ascorbate peroxidase generally respond in relation to stress to neutralize generated ROS and to maintain the redox balance within tissue system (Apel and Hirt 2004). This enzymatic defensive activity in most of the events get elevated during initial stage but with increase in preservation period, they gradually decline down (Saeed et al. 2014; Chakrabarty et al. 2009). Skutnik et al. (2021) reported increase in catalase activity with increase in content of hydrogen peroxide inside tissue system during post-harvest stage and thereby nullifying generated ROS. The catalase activity was also found to be on higher scale in cut peonies prolonging vase life and this activity was reported to be higher when preservation was carried out in solution containing nanosilver and sucrose (Rabiza-Swider et al. 2020).

Prevention of post-harvest shelf life extension was also mediated by vascular blockage caused by deposition of macromolecules preventing normal conducting pathways (Hassan 2005). Blockage of xylem lumen was also caused by microbial proliferation in the preservative solution (Zakrzewski 2009). Beside microbes and macromolecules, blockage of vascular lumen was also mediated through deposition of colloidal substances (Neumann et al. 2010). Histochemical study through microscopic observation was the most suitable way for detecting nature of vascular

blockage pattern during the course of preservation (Jedrzejuk et al. 2012). Among different preservative solutions, various studies has reported effectiveness of biogenic nanosilver solution in preventing microbial proliferation and thereby maintaining post-harvest shelf life (Maity et al. 2019; Basiri et al. 2011). Nanosilver solution can penetrate the bacterial cell membrane quite efficiently and thus displaying bactericidal effect (Yin et al. 2000). Solgi (2014) reported that efficiency of nanosilver over other chemical agents towards bactericidal activity was probably due to its large surface area.

2.4. Role of nanosilver and silver salts in senescence alteration and oxidative stress mitigation

Senescence is a pre-defined process of long term ageing in plants. Generally the process of senescence is noticeable in a plant part like leaves, branches or roots instead of entire plant for perennial plants, while in annual and seasonal plants undergoes complete senescence (Thomas 2012; Munné-Bosch 2008). In perennial plants, transport of minerals and nutrients from senescence tissue in developing tissues was a general developmental phenomenon (Maillard et al. 2015). This transportation occurs when expression of genes associated with destruction and mobilization of macromolecules increases with the onset of senescence associated stress and that for photosynthesis decreases (Buchanan-Wollaston et al. 2003). Similar expression of genes also takes place at post-harvest stage, preventing shelf life extension. In plants, appearance of senescence can be identified by yellowish leaves due to loss of chlorophyll content, degradation of proteins and low photosynthetic activity (Keles 2009). During leaf senescence, enhanced accumulation of ROS inside tissue system such as superoxide anion, hydroxyl radical, hydrogen peroxide, singlet oxygen and other harmful free radicals causes cellular damage, membrane lipid peroxidation and programmed cell death (Breusegem and Dat 2006). One of the major reasons for senescence activation in plants or plants parts like leaves was enhanced expression of ethylene hormone (Iqbal et al. 2017). The inhibitory effect of silver (Ag^+) ions on ethylene has been explored by many researchers in preventing senescence (Nejatzadeh-Barandozi et al. 2014). Ouma et al. (2004) reported the ability of silver nitrate in inhibiting ethylene biosynthesis in cotton plant. It has been reported that application of ethylene inhibitors such as silver nitrate and silver thiosulfate promotes shoot

formation by delaying the process of aging (Strader et al. 2009; Giridhar et al. 2001).

Silver nanoparticle more specifically that was synthesized using green technology bears efficiency in delaying senescence, especially in cut flowers at post-harvest stage (Rabiza-Świder et al. 2020). Karuppanapandian et al. (2011) reported that in preventing leaf senescence, silver nanoparticles are more powerful than silver nitrate. During senescence lipid peroxidation is induced, which leads to leakage of electrolytes through cell sap especially from the older plant parts. This membrane lipid peroxidation accumulates MDA during senescence, reflecting the severity of cell damage. Application of nanosilver has been reported to reduce accumulation of hydrogen peroxide and MDA in cut rose (Hassan et al. 2014). Rabiza-Świder et al. (2020) reported enhanced defensive activity through the activation of defensive enzymes like superoxide dismutase and catalase in inflorescence of cut snapdragon flowers when preserved in amalgamated solution of nanosilver and sucrose. Zhao et al. (2018) also reported preservative potentiality of silver nanoparticles through activation antioxidant defensive activity in cut peony flowers.

2.5. Proteomic analysis of mulberry leaves and silkworm larvae with special reference to gel electrophoresis

Protein is the functional molecule inside tissue system synthesized through the fundamental process of central dogma of gene expression (Kosti et al. 2016). Although genomic equivalence persist in each and every cell of a tissue system but the expression profile varies largely. Depending upon the physiological state, different cells express selective proteins that perform the cellular, molecular, and biological functions (Greller and Tobin 1999). Mulberry holds high nutritional value in terms of leaf protein that serves as feeding supplement to herbivorous group of organisms (Kandylyis et al. 2009). The leaf protein of mulberry plays vital role in the development of silk gland of the silkworm larvae (Sekar et al. 2016). 2D gel electrophoresis by the application of SDS-PAGE is the most conventional method for the detection of different cellular proteins (Ikononov et al. 1999). Through SDS gel electrophoresis Madhu Babu et al. (2014) has detected 10 – 12 protein bands in five mulberry varieties *viz.* ATP, M5, S13, S36 and V1 that have molecular mass in the range of ~18 to 97 KDa. Similarly Jyothi et al. (2016) has identified 10 – 12

protein bands in the range of ~14 to 120 KDa while working on four mulberry cultivars namely G-2, G-4, RC-1 and RC-2. Mahmoud (2017) through SDS-PAGE has reported 5 protein bands in mulberry leaves and 15 protein bands in silk gland of silkworm larvae, supplemented with same leaves. Chaitanya et al. (2001) has reported the appearance of additional two protein bands of 68 and 85 KDa under heat stress, proving differential expression of proteins under stress. SDS-PAGE has identified haemolymph proteins in silkworm larvae in the range of 30 to 80 KDa, participating in various metabolic processes including moulting (Hou et al. 2010). Bhat et al. (2014) on performing gel electrophoresis of middle silk gland has identified heavy and low chain fibroin protein of molecular mass 325 and 26 KDa respectively. Dong et al. (2016) on performing LCMS/MS analysis of silk gland proteins has identified ~1271 proteins which through GO annotation via Blast2GO tool has detected the presence of proteins that are involved in the process of transportation, stress response, signalling mediator, and metabolic and cellular organization. For the management of generated stress inside tissue system, activation of series of defensive enzymes takes place. Some enzymes act as stress markers, while some other functions are associated in the direction of stress mitigation. NADPH oxidase is a crucial stress marker whose enhancement in activity leads to overproduction of ROS inside cellular organization (Marschall et al. 2016). While enzymes like SOD, CAT and POD functions as stress inhibitors as they nullifies excess generated ROS and maintains homeostasis inside the body of an organism (Nandi et al. 2019; Fukai and Ushio-Fukai 2011). Hirano and Naganuma (1979) through isozyme profiling have reported the presence of well defined peroxidase activity within mulberry leaves that nullifies generated ROS. Hirano (1977) through isozyme profiling has reported the presence of five isoforms of peroxidase isozyme in mulberry leaf blade. Tewari et al. (2010) has reported increased activity of CAT, SOD, POD and APX in boron-deficit mulberry leaves. Thus through detection and study of differentially expressed protein and isozyme banding pattern one can predict the internal physiological changes that takes place with the onset of stress and its defensive strategies.

2.6. Next-generation sequencing with special reference mulberry and cellular senescence

Next-generation sequencing (NGS) is a latest advancement towards obtaining sequence of DNA and RNA and detection of differential expression, variation and mutation within and among species (Qin 2019). It is a rapid process that can sequence the entire set of genome in an organism in a time interval of few hours (Behjati and Tarpey 2013). Genomic information of mulberry is crucial for the development of superior quality cultivar having high yield and nutritional efficiency. Vijayan (2010) has stated that transcriptome analysis through next generation sequencing will help molecular breeders to develop high yielding mulberry cultivars for greater acceptability by silkworm larvae. Wang et al. (2018) has reported 112,481 transcripts through *de novo* assembly by using Illumina platform from ~16 Gb raw RNA sequence data of *Morus alba*. Similarly, Guan et al. (2018) through Illumina Hiseq2000 platform reported 133,002 *de novo* assembled transcripts of *Morus alba* leaves that was subjected to high-level UV-B exposure. Chen et al. (2015) has reported 158,680 bp circular chloroplast genome of *Morus notabilis* through Illumina sequencing.

Progressive deterioration of cellular and sub-cellular components with ageing is termed as senescence. While senescence that get imposed with the onset of stress is termed as premature senescence and it causes serious problem in maintaining productivity of agricultural crops and often result in economic losses. Identification and detection of genes and mechanistic pathways responsible for acceleration of premature senescence might help to put a check over low crop yield by imposition of stress. Zhao et al. (2018) through transcriptome analysis has identified four senescence related pathways including hormonal and chlorophyll metabolism responsible for appearance of premature senescence in *Nicotiana tabacum*. Chao et al. (2018) while studying mechanism of leaf senescence in legume plants (*Trifolium pratense*) through RNA sequencing technology has identified 207 genes that played direct role in promoting senescence. Transcriptome analysis of leaf senescence in *Medicago truncatula* under salt stress has identified 4,419 senescence related genes (Dong et al. 2021). Differential expression of genes through RNA sequencing technology has identified 52,382 and 6680 up- and down-regulated genes between fresh and senescence leaf of *Cynodon dactylon* (Fan et al. 2019). Kim et al. (2018) while studying comparative transcriptome associated with leaf senescence in *Arabidopsis* has identified two antagonistic plant hormone *viz.* ethylene (senescence

promoter) and cytokinin (senescence inhibitor). Thus Illumina tool plays a significant role in comparative analysis of genomic sequences that provides next generation platform for detecting probable cellular, molecular and biological pathways associated with a particular physiological response.

During construction of the review, it has been found that sufficient information in the form of published papers is available regarding green synthesis of silver nanoparticles. Among different types of extracts used for the preparation of silver nanoparticles, green mature leaves of angiosperms were mostly used. It was observed that the size of the nanoparticles formed varied widely from one species to another. Different type of biomolecules that are present in plant extract helps in reducing silver ion to nanosilver. The green synthesized nanoparticles showed their great potentiality as antioxidant, and antimicrobial agent; beside this application of nanoparticles was confirmed for extending shelf-life of horticultural crops, in preservation of processed food, and medicine industry. Thus, from overall viewpoint, green synthesized nanosilver displayed great potential than nanoparticles synthesized through physical and chemical methods and its utility is developing in the field of science with wider range of applications in near future.